Title

Interannual differences in larval haddock survival: hypothesis testing with a 3D biophysical model of Georges Bank

Journal

Fisheries Oceanography, 23(6)

ISSN

1054-6006

Authors

Petrik, Colleen M
Ji, Rubao
Davis, Cabell S

Publication Date

2014-11-01

DOI

10.1111/fog.12087

Peer reviewed

Interannual differences in larval haddock survival: hypothesis testing with a 3D biophysical model of Georges Bank

COLLEEN M. PETRIK*,[1], RUBAO JI, CABELL S. DAVIS

Biology Department, Woods Hole Oceanographic Institution, Woods Hole, MA 02543

*corresponding author: cpetrik@ucsc.edu

[1]Present affiliation: Institute of Marine Sciences, University of California Santa Cruz. Present address: NOAA NMFS Southwest Fisheries Science Center, 110 Shaffer Rd. Santa Cruz, CA 95060

ABSTRACT

The ultimate goal of early life studies of fish over the past century has been to better understand recruitment variability. As evident in the Georges Bank haddock (*Melanogrammus aeglefinus*) population, there is a strong relationship between recruitment success and processes occurring during the planktonic larval stage. This research sought new insights into the mechanisms controlling the recruitment process in fish populations by using biological-physical modeling methods together with laboratory and field data sets. We created the first three-dimensional model of larval haddock on Georges Bank by coupling models of hydrodynamics, lower trophic levels, a single copepod species, and larval haddock. Interactions between feeding, metabolism, growth, vertical behavior, advection, predation, and the physical environment of larval haddock were quantitatively investigated using the coupled models. Particularly, the model was used to compare survival over the larval period and the sources of mortality in 1995 and 1998, two years of disparate haddock recruitment. The results of model simulations suggest that the increased egg hatching rates and higher food availability, which reduced starvation and predation, in 1998 contributed to its larger year-class. Additionally, the inclusion of temperature-dependent predation rates produced model results that better agreed with observations of the mean hatch date of survivors. The results from this biophysical model imply that food-limitation and its related losses to starvation and predation, especially from hatch to 7 mm, may be responsible for interannual variability in recruitment and larval survival outside of the years studied.

Keywords: larval fish, individual-based model, recruitment, GLOBEC

INTRODUCTION

The annual variation in year-class size of a fish population can greatly influence the biomass of the population that can be fished (Trippel & Chambers, 1997). Despite its importance, the causes of recruitment variability are not clear, and understanding recruitment variability has long been a goal to aid in the management of fisheries. Since Hjort's (1914) hypothesis that the size of a year-class is determined during the early life stage of fish, much emphasis has been placed on survival from the egg to the early juvenile stage. The haddock, *Melanogrammus aeglefinus*, population on Georges Bank (Fig. 1) has the classic dependence on intense but sparse recruitment years and also is known to have a strong relationship between recruitment and processes occurring during the larval stage (Mountain *et al.*, 2008).

Larval haddock had greater survival when mismatched (phase-shifted) to the copepod populations for the years 1995-1999 (Buckley & Durbin, 2006). By hatching before the spring bloom, haddock maximized size at time of year rather than size at age (Lapolla & Buckley, 2005; Buckley & Durbin, 2006; Buckley *et al.*, 2010). Though hatching early results in slower growth from lower temperatures, less food, and less light available for visual feeding compared to later in the year, it leads to less predation as well (Lapolla & Buckley, 2005; Buckley & Durbin, 2006; Buckley *et al.*, 2010). These findings appear to contradict the larval fish paradigms about size and survival, specifically that individuals with higher growth rates will spend less time as vulnerable larvae, particularly small larvae, with high mortality rates (Leggett & Deblois, 1994). However, if changing climate conditions lead to higher prey availability earlier in the year (Ji *et al.*, 2008), survival of early-spawned larvae could be further enhanced. In

addition to seasonal prey availability and predation risk, advection could be important in regulating the recruitment of haddock. Advective loss of larvae or their planktonic copepod prey could occur early in the spawning period before the gyre has strengthened with seasonal stratification (Butman & Beardsley, 1987), as well as from Gulf Stream rings (Butman *et al.*, 1982; Flierl & Wroblewski, 1985), and strong wind events (Chase, 1955; Lewis *et al.*, 1994, 2001).

Spatially-explicit coupled biological-physical individual-based models (IBMs) are ideal for studying the processes of feeding, growth, predation, and advection during the larval stage. Such models act as laboratories where simulation experiments can be conducted to disentangle these factors, determine their relative importance, and reveal how they are affected by environmental variability. We seek to gain insights into the recruitment variability of Georges Bank haddock by using a spatially-explicit coupled biological-physical IBM to examine two disparate years sampled during the U.S. GLOBEC Northwest Atlantic/Georges Bank (GLOBEC GB) program during 1995-1999 (GLOBEC, 1992; Wiebe *et al.*, 2002). The 1998 haddock year-class was the largest of the study period and the largest since 1978, until the record 2003 year-class (Brodziak & Traver, 2006) that outsized the previous record 1963 year-class. The 1998 year-class had a broad spawning period, low egg production, and the highest egg and larval survival rates of the five GLOBEC study years (Buckley & Durbin, 2006; Mountain *et al.*, 2008). On the other hand, 1995 was a year of low recruitment with low prey biomasses (Buckley & Durbin, 2006) resulting in food-limited growth and the condition of some first feeding haddock larvae indicative of starvation (Buckley *et al.*, 2006). In addition to recruitment,

both recruitment per hatched egg (Mountain & Kane, 2010) and larval abundance at 15 days post hatch (Mountain *et al.*, 2008) were higher in 1998 than 1995.

We coupled a hydrodynamics model, a nutrient-phytoplankton-zooplankton-detritus (NPZD) model, a stage-based copepod population model, and a larval haddock IBM to simulate the processes on Georges Bank during the larval period of haddock. The model was used to compare survival over the larval period and the sources of mortality in 1995 and 1998. As stated above, there are generally three hypothesized sources of larval mortality: advection, predation, and starvation. These hypotheses were tested to see if any accounted for the observed differences between 1995 and 1998. Specifically, we tested the role of hatch location and abundance, the physical environment, prey density, vertical swimming behavior, seasonal predation, spatial predation, and interannually-varying predation.

METHODS

Physical model

The hydrodynamics were provided by the Finite Volume Coastal Ocean Model (FVCOM). FVCOM is a prognostic, unstructured-grid, finite-volume, free-surface, three-dimensional (3D), primitive equation coastal ocean circulation model (Chen *et al.*, 2003). FVCOM receives input from an atmospheric model (Fifth-Generation Penn State/NCAR Mesoscale Model, MM5), is driven by realistic surface and boundary forcing, and assimilates satellite and buoy data. There is a Lagrangian particle-tracking routine for FVCOM, which can be used to couple individual-based biological models (Chen *et al.*, 2006; Ji *et al.*, 2012). The particle-tracking routine was run offline with FVCOM output saved every hour as the physical forcing. Preliminary tests demonstrated that daily output was too coarse and resulted in different trajectories compared to hourly, which captured the important tidal circulation on Georges Bank. Chen (1992) estimated the auto-correlation time scale of currents on Georges Bank as one hour, using 5 min ADCP data recorded in the Great South Channel. Thus, velocities at time scales shorter than one hour are coherent, and there was no need to use FVCOM flow output at a higher temporal resolution than hourly. Additionally, hourly output of FVCOM results have been applied to the Gulf of Maine and Georges Bank region (Huret *et al.*, 2007; Churchill *et al.*, 2011) and the resulting trajectories captured the general transport patterns well.

The saved velocities were used to calculate Lagrangian pathways by linear interpolation in space and time, with an explicit fourth order Runge-Kutta scheme and a time step of 30 s. A random walk model was applied to simulate vertical diffusion by applying the method of Visser (1997) using the FVCOM-saved vertical velocity and

138 vertical eddy diffusivity that was calculated with the Mellor and Yamada (1982) level 2.5
139 turbulence closure model. This random walk model is sensitive to the time step, thus a
140 smaller time step of 0.2 s was necessary for the random walk process to prevent specious
141 particle accumulation in areas of low diffusivity. In addition to velocity and diffusivity,
142 temperature, light, and bottom depth from FVCOM were also stored and used in the
143 biological submodels.
144
145 *Prey field*
146 Many IBMs use size-based feeding models, however it has been shown that larval fish
147 prey selection is not purely size-based (Petrik *et al.*, 2009). Copepod prey of similar size
148 are ingested in amounts disproportionate to their abundance in the environment (Kane,
149 1984; Heath & Lough, 2007). In addition to its size, the behavioral properties of the
150 copepod *Pseudocalanus* spp. make it the most preferred prey item of larval haddock
151 (Petrik *et al.*, 2009). It is the majority of the prey biomass consumed (Kane, 1984, Lough
152 *et al.*, 2005; Heath & Lough, 2007) and its biomass is highly correlated to larval haddock
153 growth rate (Buckley & Durbin, 2006). As a simplification, *Pseudocalanus* spp. was used
154 as the sole prey source to larval haddock in the coupled model. The *Pseudocalanus* spp.
155 density was modeled with a 4-stage (eggs-nauplii-copepodite-adult) concentration-based
156 population model (Hu *et al.*, 2008; Ji *et al.*, 2009), excluding the eggs as a prey source.
157 The FVCOM hydrodynamics model was coupled to a NPZD model, with the flow fields,
158 temperature, and phytoplankton serving as inputs to the copepod population model (Ji *et*
159 *al.*, 2009). These runs were completed prior to the haddock IBM simulations, with the

160 resulting *Pseudocalanus* spp. concentrations stored every hour and used as offline prey
161 inputs.
162
163 *Larval haddock IBM*
164 The following descriptions are all components in the IBM of larval haddock within the
165 offline FVCOM particle tracking routine. These processes occurred with a time step of 15
166 min. For complete equations and parameterizations, see the Appendix.
167
168 Super-individuals
169 To simulate realistic numbers of individuals and prevent significant variation
170 from being lost from the population, super-individuals (Scheffer *et al.*, 1995) were used
171 to represent larvae. The number of individuals, *n*, within each super-individual was
172 determined from estimated egg hatching rates calculated for the years 1995 and 1998 on
173 Georges Bank (Mountain *et al.*, 2003, 2008). Daily estimates of egg hatching rates were
174 spatially interpolated to a regular grid covering the sampling area (Mountain *et al.*, 2003,
175 2008), with roughly 1955 grid nodes within the 200 m isobath used to define Georges
176 Bank in this study. Egg hatching rates in units of no. 10 m^{-2} d^{-1} were converted to total
177 number of individuals hatched per month by multiplying the rate by the area covered by
178 that grid box and the total number of days in that month. Depending on cohort and year,
179 this method resulted in hatching at 890-1874 of the grid cells with various numbers of
180 individuals. The center of each grid box was the location each super-individual was
181 released at hatch. The number of super-individuals necessary to produce stable results
182 was tested by releasing 1, 2, or 3 super-individuals at each grid node with estimated egg

183 hatching. For each test case, the reference model (see *Simulations* section below) was run
184 and summary metrics (see *Analyses* section below) were calculated. Data for untested
185 numbers of particles was added to these graphs by randomly subsampling the model
186 output with 3 super-individuals per node 100 times for each number that was not
187 simulated. The minimum number of particles needed was equivalent to the asymptotes of
188 the graphs of metric as a function of particle number. Asymptotes were defined as when
189 the mean of 100 subsamples fell within one standard deviation of the results with the
190 greatest number of particles subsampled. The simulated results and the mean results of
191 random subsamples converged when particles >2250. The final numbers used in all
192 simulations were $2.67\times10^3 - 5.63\times10^3$ super-individuals with $6.43\times10^5 - 2.42\times10^{10}$
193 individuals per super-individual (Table 1). These amounts are similar to the numbers of
194 particles simulated by Huret *et al.* (2007) with FVCOM in the Gulf of Maine, who
195 independently performed a stability analysis.
196
197 Foraging submodel
198 The foraging submodel (Appendix eqs. 1-16) was based on the larval fish feeding
199 models of Caparroy *et al.* (2000) and Fiksen and MacKenzie (2002), adapted for cod by
200 Kristiansen *et al.* (2007) and parameterized for larval haddock and *Pseudocalanus* spp.
201 by Petrik *et al.* (2009). Ingestion was the product of encounter rate and the probability of
202 successful capture. Encounter rate was a function of prey density, prey swimming speed,
203 turbulent velocity, larval fish pause duration and frequency, and larval perception
204 distance (dependent on light and larval size). The probability of successful capture was an
205 empirical function of copepod species (*Pseudocalanus* spp.) and developmental stage

206 length parameterized from mechanistic simulations of species-specific copepod escape
207 behaviors, including the deformation rate threshold, escape jump speed, and escape jump
208 angle. The species-specific prey characteristics were also size-specific, however size was
209 not a state variable in the copepod population model. As a first approach, the length,
210 width, and biomass of a grouped developmental stage (e.g. nauplii) was set as the mean
211 of all stages within that group (e.g. mean of NI-NVI) using the lengths, widths, and
212 biomasses in Davis (1984, 1987). This empirical function was used to reduce computing
213 time instead of simulating 10^2-10^5 iterations of each larva trying to capture each prey item
214 at each time step to calculate the probability of successful capture as was done in Petrik *et*
215 *al.* (2009).
216
217 Bioenergetics submodel
218 The bioenergetics submodel (Appendix eqs. 17-33) was the same as that used in
219 Petrik *et al.* (2009) for larval haddock, which was based on Kristiansen *et al.* (2007) for
220 larval cod. The energy derived from the amount of biomass ingested in the foraging
221 submodel was apportioned to metabolism and growth, both of which were temperature-
222 and larval size-dependent. Metabolism was increased a constant amount during light
223 hours to account for the swimming activity of feeding fish. The light threshold was
224 updated to reflect the findings of Vollset *et al.* (2011) of active feeding at low light
225 intensities. The light threshold changed from 1.0×10^{-3} μmol m^{-2} s^{-1} for all sizes, to
226 5.0×10^{-3} μmol m^{-2} s^{-1} for larvae <7.5 mm and 5.0×10^{-4} μmol m^{-2} s^{-1} for larvae ≥7.5 mm.
227
228 Predation submodel

229 Interactions with individual predators were not modeled, but both visual and
230 nonvisual predators were represented by predation rates (Appendix eqs. 34-39).
231 Nonvisual predation, representative of ambush or tactile invertebrate predators, was
232 assumed to be a decreasing function of larval fish (their prey) size. The nonvisual
233 predation rate was found using a size-dependent model adapted from Peterson and
234 Wroblewski (1984) and was constant spatially and temporally for a given size.
235 Visual predators were simulated by following the visual predation models of
236 Aksnes and Giske (1993), Aksnes and Utne (1997), and Fiksen & Jørgensen (2011).
237 Visual predator density was assumed to decrease with increasing larval size since the size
238 of the predator must increase, and larger animals tend to have lower densities than
239 smaller ones (Sheldon *et al.*, 1972; Jennings & Mackinson, 2003). The visual predation
240 rate decreased with larval size and depth, but was constant horizontally and in time.
241 The total base predation rate was the sum of nonvisual and visual predation rates.
242 The visual predation rate was parameterized such that the total base predation rate was
243 approximately 0.1 d^{-1} for a 5 mm larva (Bailey & Houde, 1989). Similar to the visual
244 predation rate, the total predation rate decreased with larval size and depth, and was
245 constant horizontally and in time.
246
247 Mortality
248 Mortality of larvae resulted from starvation, advection, or predation. Entire super-
249 individuals were removed from the population if they starved or were lost to advection. A
250 larva was considered to have starved to death if its mass fell below 70% of the mass that
251 it would have at that length under unlimited food conditions (Kristiansen *et al.*, 2009;

252 Appendix eq. 33). Since all individuals within a super-individual were identical
253 biologically, starvation of a super-individual resulted in loss of all of its individuals.
254 Similarly, if a super-individual was lost to advection, then all of its individuals were lost
255 because they all have the same location in time and space. Super-individuals were
256 deemed lost by advection when they crossed the 200 m isobath (Fig. 1). The 200 m
257 isobath has been used to define the edge of Georges Bank in other studies that estimated
258 bank residence times (Colton & Anderson, 1983; Page *et al.*, 1999) and retention of
259 larval fish (Lough *et al.*, 2006). Advective loss served as a proxy for the combination of
260 starvation that would occur as the larvae left the rich prey environment of the bank,
261 predation by mesopelagic fishes off the slope of the bank, and the inability to find
262 suitable juvenile settlement habitat.
263 As argued by Scheffer *et al.* (1995), losses of individuals within a super-
264 individual via predation were modeled by drawing a random number from a binomial
265 distribution (Appendix eqs. 51-55). The probability of predation, p, for a super-individual
266 was calculated from an exponential probability distribution from the total predation rate.
267 This probability was used with an exact binomial probability density function when
268 $n \leq 20$. To reduce computation time, approximations for the binomial distribution were
269 used when $n > 20$. When $n > 20$ and $np \leq 50$, the Poisson approximation for a binomial
270 distribution with small p was used. The Poisson distribution was further approximated by
271 a normal distribution when $n > 20$ and $np > 50$. At each time step, n was reduced by the
272 number drawn from the binomial or binomial approximated probability distribution.
273
274 *Simulations*

Two contrasting years in haddock recruitment, 1995 and 1998, as observed during the GLOBEC GB field study, were chosen for this modeling study. Super-individuals were initialized as newly-hatched 5 mm larvae in the number and location specified from the egg hatching rate estimates of each year. Hatch locations were determined from observations of egg abundance (Sibunka *et al.*, 2006) projected forward using estimated egg mortality rates and spatially integrated using kriging as described in Mountain *et al.* (2003, 2008). Initial depth was random from surface to bottom to approximate the uniform distribution of eggs from wind and tidal mixing (R. G. Lough, NOAA NMFS NEFSC, USA, pers. comm.). Three different cohorts were simulated each year, which hatched on the midpoint of February, March, and April. Simulations were run until mid-June, the last month sampled by the GLOBEC GB surveys in 1995. Thus, the run time of the April cohort was 55 d. For equality, each cohort was analyzed until 55 days post hatch (dph). Analyses were made at 55 dph or at the time when larvae reached 12 mm, the average length at the transition to pelagic juveniles, if that occurred before 55 dph. It was assumed that the model no longer applied to juveniles because they have different metabolisms, are less vulnerable to predation, and have greater swimming abilities. The model timespan of 55 dph was deemed an adequate representation of the larval period since the time of transition from pelagic juveniles to demersal juveniles (which occurs after the transition from larvae to pelagic juveniles) has been estimated as 2 months (Page *et al.*, 1999; Mountain *et al.*, 2003). Because the mortality calculations include individuals that survived the first 55 dph, but did not reach 12 mm, the analyses represent the processes acting during the majority of the larval period, and not up until the exact time of juvenile transition.

298 A total of 19 different simulations were run, 9 for 1995 and 10 for 1998 (Table 2).
299 The reference case used the model in its simplest form to contrast larval survival in 1995
300 and 1998. The additional simulations can be considered as hypothesis tests or sensitivity
301 analyses. They were performed to test whether additional information was necessary to
302 replicate the hatch dates of survivors and the survival differences between 1995 and
303 1998.
304
305 Reference case (R)
306 As a reference case, super-individuals were modeled as passive (neutrally
307 buoyant) particles. All other model components were as described above.
308
309 Opposite environment (O)
310 To distinguish the effect of the environment during transport from that of hatch
311 locations and abundance, the locations and numbers of one year were used in conjunction
312 with the physical (velocity, temperature, light) and biological (prey density) environment
313 of the other year.
314
315 Low prey (L)
316 The spatial and temporal patterns in *Pseudocalanus* spp. abundance from the
317 population model match climatological observations (Ji *et al.*, 2009). The tempo-spatial
318 patterns from a preliminary model run for *Pseudocalanus* from 1995-1999 also agreed
319 with yearly observations, but the absolute abundances for 1998 were lower than
320 observed. The observed abundance of *Pseudocalanus* in 1998 was 2-3 times higher than

321 that in 1995 (Ji *et al.*, 2012). To account for this, the 1998 copepod model concentration
322 was increased by a factor of 5 to result in mean abundances 2-3 times higher than the
323 1995 output from the copepod model in the reference case and all other cases. In the
324 “low-prey" simulation the 1998 densities were only increased by a factor of 2.5 to
325 approximate the 1995 prey densities and to test if prey density was the cause of
326 differential survival.
327
328 Swimming behavior (DVM)
329 Since the mechanism responsible for larval haddock depth selection has not been
330 resolved, a simple vertical behavior was simulated to test its effect on survival. Lough
331 and Potter (1993) observed a diel difference in vertical distribution of larvae 9 mm and
332 larger. The diel vertical migration (DVM) behavior simulations imposed preferred
333 daytime and nighttime depths of 40 m and 20 m, respectively, for larvae >9 mm
334 following observations. Daytime was regarded as when surface light (from the physical
335 model) was $>1.0\times10^{-3}$ μmol m^{-2} s^{-1}. Vertical swimming velocity was implemented as a
336 tangential function that directed larvae towards the preferred depth (Appendix eqs. 56-
337 57). The swimming speed was symmetric about the preferred depth. Above it the velocity
338 was negative so that larvae swam down; below it the velocity was positive so that larvae
339 swam up. Speed decreased as a super-individual neared the preferred depth.
340
341 Temperature-dependent predation (TP)
342 Following Houde (1989), the temperature-dependent predation rate increased 0.01
343 d^{-1} per 1°C increase in temperature (Appendix eqs. 40-42). The base temperature was set

344 as 6.5°C, the temperature associated with the predation rate of 0.1 d^{-1} for a 5 mm larva
345 (Jones, 1973; Bailey & Houde, 1989; Houde, 1989). A second temperature-dependent
346 predation simulation was run with a lower base temperature (5.5°C), which caused even
347 greater predation rates during warmer months. Both forms were used to test if higher
348 predation rates in the late spring would result in more survivors from the early hatch
349 dates as observed.
350
351 Spatially-dependent predation (CP, FP)
352 The distribution of potential predators of larval haddock on Georges Bank (e.g.
353 chaetognaths, predatory copepods, amphipods, mysid shrimps, decapod shrimps,
354 euphausiids, hydroids, hydromedusae, scyphomedusae, siphonophores, herring,
355 mackerel) falls into two groups, those that are more abundant on the shallow, well-mixed
356 crest region (shoalward of the 60 m isobath; C in Fig. 1), and those that are more
357 abundant on the seasonally stratified flanks that are in waters deeper than 60 m (e.g. NF
358 and SF in Fig. 1). The predators are more diverse and abundant on the crest (Sullivan &
359 Meise, 1996), however this does not necessarily equate to higher predation rates because
360 of possible differences in consumption rates. Two different simulations were run to test
361 the effect of spatially-dependent predation, one where predation was three times as high
362 on the crest compared to the flanks, and a second where predation was higher on the
363 flanks (Appendix eqs. 43-46). Predation rates were offset from the base predation rate by
364 ±50% to keep predation losses comparable to simulations that did not have spatially-
365 dependent rates.
366

Interannually varying predation (95P+, 95P-)

We varied the predation rates in 1995 and 1998 to investigate the hypothesis of dissimilar rates from any combination of different predator communities, abundances, and consumption rates between the two years. The base predation rate was altered by ±10% in one year and by ±10% in the opposite direction in the other (Appendix eqs. 47-50). The results presented are as the variation made to the 1995 simulations (e.g. 95P+ or P+ is 10% higher in 1995 and 10% lower in 1998).

Analyses

Starvation, predation, and advection fatalities were calculated as the fraction of individuals hatched in each cohort that were lost to that source of mortality before 55 dph or upon reaching 12 mm. Similarly, percent survival was assessed as the number of individuals hatched in each cohort that were alive at 55 dph or upon reaching 12 mm. To better discriminate the sources of mortality affecting larval survival in the model simulations, percent loss to different sources was analyzed in a systematic way to isolate the impact of each. This approach allowed distinguishing between whether loss to one source of mortality was reduced/increased because of its driving factors (i.e. prey abundance, predation rate, etc.) or because the other sources of mortality were increased/reduced.

In addition to the fractions of each cohort that survived or were lost to different sources of mortality, hatch distributions, cohort contributions, and survival per hatch were also calculated from model results. The hatch distribution of each year was the fraction of individuals hatched in each month out of the total hatched that year. The

390 contribution of each cohort to survivors represented the percent of survivors from each
391 hatch date out of the total number of survivors from all hatch dates in one year combined.
392 Hatch distribution and cohort contribution analyses were repeated for larvae that hatched
393 on the western and eastern sides of Georges Bank separately. Cohort contributions were
394 compared to the estimated hatch dates of juvenile survivors collected in the field (Lapolla
395 & Buckley, 2005; Mountain *et al.*, 2008). The total annual percent survival was the total
396 number of survivors from all hatch dates out of the total number of individuals hatched in
397 that year, and is termed "survival per hatch." The survival per hatch ratio compared the
398 survival per hatch value of 1998 to that of 1995 for each simulation. Model survival per
399 hatch was compared to recruits per hatch estimated from observations (Mountain &
400 Kane, 2010).
401 Cohort and year means were calculated for each simulation for the following
402 properties: time to 12 mm, specific growth rate, depth, temperature experienced, and prey
403 concentration experienced. Mean depth was calculated for all individuals and those that
404 survived to 12 mm, whereas means of time to 12 mm, specific growth rate, temperature,
405 and prey concentration were only calculated for individuals that survived to 12 mm.
406 Means of growth rate, temperature, and prey concentration accounted for the time from
407 hatch until each individual reached 12 mm. All results were analyzed at the level of
408 individuals within the super-individuals. A weighted mean, the mean of the super-
409 individuals weighted by the number of live individuals within each super-individual, was
410 used since these properties were shared by all individuals within a super-individual.
411
412

RESULTS

Reference case

Larval distributions

Distributions of larvae at hatch differed between months and years in the passive, reference simulations (Fig. 2a-c, 3a-c). In February of 1995, larvae hatched on both the eastern and western sides of the bank, with none in the middle (Fig. 2a). In March 1995, larvae were missing from the very center crest and center Southern Flank (SF; Fig. 2b), whereas hatching in April was restricted to the east side and along the SF (Fig. 2c). The majority of larvae hatched in February 1998 were on the eastern side of the bank, with some on the NW side (Fig. 3a). March 1998 hatch distributions surrounded the perimeter of the bank, but were not in the very center of the bank (Fig. 3b), while in April, larvae hatched all over the bank (Fig. 3c).

The final distributions of all individuals, dead or alive, at the mean time that cohort reached 12 mm (Table 3) varied between months and years because of disparities in initial locations and advection (Fig. 2d-f, 3d-f). In 1995, larvae of all cohorts were absent from the Northern Flank (NF; Fig. 2d-f). In contrast, larvae in 1998 were more abundant and widespread in the Mid-Atlantic Bight (MAB), demonstrative of stronger advection (Fig. 3d-f). This advection to the southwest through the Great South Channel (GSC) increased with hatch date in both years (Fig. 2d-f, 3d-f).

The distributions of 12 mm survivors (Fig. 2g-i, 3g-i) indicated the final locations of individuals that were transported through favorable environments, and were small fractions of the areas covered by the final distributions of all larvae. In 1995, survivors of all cohorts were confined to the bank crest, and the area occupied increased with hatch

436 date (Fig. 2g-i). The February and March 1998 cohorts followed this pattern, but the
437 April cohort was located in the MAB and in most areas on the bank except the SF (Fig.
438 3g-i). The area spanned by survivors from the 1998 cohorts exceeded that of the
439 corresponding 1995 cohorts (Fig. 2g-i, 3g-i).
440
441 Mortality
442 When only advective loss was considered (no starvation, no predation), advection
443 resulted in 3-13% of losses in 1995 and 6-27% in 1998 (Table 4). Losses to advection
444 were greatest for the March cohort in 1995 and the April cohort 1998, but the
445 contribution of these cohorts to total survival in each year was still the highest (Table 4)
446 because of their large numbers of larvae (Table 1). Survival per hatch was higher in 1995
447 than 1998 (Table 4).
448 When larvae were allowed to starve to death, the fraction of larvae lost to
449 advection did not change for any cohort or year (Table 4). Starvation greatly affected
450 survival, reducing it from 87-97% to 8-45% in 1995, and from 73-94% to 12-41% in
451 1998 (Table 4). Adding starvation resulted in a positive relationship between percent
452 survival and hatch date, and altered the contribution of each cohort to total survivors such
453 that later hatch dates contributed more (Table 4). Starvation losses reversed the survival
454 per hatch pattern between years to be greater in 1998 than in 1995 (Table 4).
455 When predation mortality was taken into account, percent survived, advected, and
456 starved all decreased (Table 4). In general, predation was a greater source of mortality to
457 larvae that would have starved than to larvae that would have been lost to advection. The
458 patterns of the greater survival per hatch in 1998 and of increasing cohort contribution

459 with hatch date in both years remained unchanged, and the contributions of the April
460 cohorts were intensified (Table 4). Survival per hatch decreased from 23-29% due to
461 advection and starvation only, to 1-2% with the addition of predation mortality (Table 4).
462
463 Cohort survival
464 A greater number of larvae hatched in all months of 1998 compared to 1995
465 (Table 1). In 1998, the April cohort made up the largest proportion of larvae hatching and
466 surviving, and the February cohort the least (Fig. 4 right). Conversely, the majority of
467 larvae hatching in 1995 came from the March cohort, but the proportion of survivors that
468 originated in the April cohort was greater than the proportion of all hatched larvae
469 derived from that cohort (Fig. 4 left).
470 Percent survival increased with cohort hatch date in both 1995 and 1998 (Table
471 4). Percent survival of all the 1995 cohorts was lower than the respective 1998 cohorts
472 (Table 4). The 1998 April cohort had the highest percent survival (Table 4) and the
473 greatest number of surviving individuals (Table 5). Starvation losses decreased with
474 hatch date for both years, while advection losses increased (Table 4). In 1995, predation
475 losses were highest and equal for the March and April hatch dates, whereas loss to
476 predation increased with hatch date in 1998 (Table 4).
477
478 Growth rates
479 The weighted mean time to 12 mm (d) decreased with increasing cohort hatch
480 date for both years, however weighted mean specific growth rates (d^{-1}) of 12 mm
481 survivors did not increase with hatch date (Table 3). Mean time included individuals that

482 reached 12 mm after the 55 d larval period, but mean growth did not. The March cohort
483 had the fastest growth rates in 1995 and the slowest in 1998, when the April cohort had
484 the highest (Table 3). The mean time was shorter and mean growth rate faster for the
485 February and April cohorts in 1998 compared to the corresponding cohorts from 1995,
486 but the March cohorts had equivalent mean times and growth rates (Table 3). Since the
487 mean temperatures experienced by the surviving larvae of the February and April cohorts
488 in 1998 were similar to those experienced in 1995 (Table 6), the faster growth rates in
489 1998 can be attributed to higher prey concentrations experienced by these larvae (Table
490 7). The mean temperatures experienced by the April cohorts were near the optimal
491 temperature for larval haddock growth under food-limited conditions (7°C; Buckley *et*
492 *al.*, 2004), while the other cohorts were below optimal (Table 6). Despite the lower
493 temperatures (Table 6) and prey concentrations (Table 7) experienced by the March 1995
494 cohort, the mean growth rate was higher than that of the April cohort, suggesting
495 selection pressure from predation, possibly from the shallower distribution of the cohort
496 in the water column (discussed in *Alternate hypotheses*-Mean depth section below).
497
498 *Alternate hypotheses*
499 Mean depth
500 Weighted mean depths were used to compare depth distributions between passive
501 (reference case, R) and vertically migrating (DVM case) larvae, between years, and
502 between all individuals and only those that survived to 12 mm. The weighted mean depth
503 of the largest fraction of all larvae was between 30 and 40 m, regardless of passive or diel
504 vertical behavior, for all hatch dates and years (Fig. 5a,c,e,g). The depth distributions of

505 all passive larvae and all larvae with behavior were very similar with slight differences by
506 cohort (Fig. 5a,c,e,g). Of the larvae that survived to 12 mm, the weighted mean depth of
507 the largest fraction, either 20 or 30 m, was higher in the water column than all larvae. The
508 passive and DVM surviving larvae from 1995 showed similar depth distributions for the
509 April cohorts, but the February and March cohorts differed (Fig. 5b,d). The passive
510 larvae from February and March 1995 had sharp maxima at 30 m while the larvae with
511 DVM had broader maxima between 20 and 30 m (Fig. 5b,d). Regardless of passive or
512 DVM, the 1995 February and March cohorts had greater fractions higher in the water
513 column than the April cohort. In 1998, survivors of the March and April cohorts had
514 similar depth distributions with or without DVM (Fig. 5f,h), and in contrast to the 1995
515 population, the passive February cohort was slightly more broadly distributed than the
516 individuals from February with DVM (Fig. 5f,h). The proportion of surviving individuals
517 at depth gradually increased with hatch date with or without vertical swimming behavior
518 in 1998 (Fig. 5f,h).

519 Comparing between years, the 1995 February and March cohorts had greater
520 proportions of all larvae with and without DVM around 30 m compared to 1998, while
521 the 1995 April cohort had fewer proportions near this depth than in 1998 (Fig. 5a,c,e,g).
522 The passive and behaving larvae that survived to 12 mm from the February cohort were
523 in higher proportion at 30 m in 1995, whereas there was a higher proportion at 20 m in
524 1998 (Fig. 5b,d,f,h). The DVM larvae that survived to 12 mm from the March cohort
525 were in greater abundance higher in the water column in 1995 compared to 1998 (Fig.
526 5d,h). Conversely, the April cohort survivors from 1995 were deeper than the 1998
527 cohort, both passive and with behavior (Fig. 5b,d,f,h).

528 The greatest differences in depth distributions were between all larvae and only
529 those that survived to 12 mm. The 12 mm survivors from all cohorts were generally more
530 abundant above 50 m (Fig. 5b,d,f,h), while all larvae had greater fractions below 50 m
531 (Fig. 5a,c,e,g). In all comparisons, there was a steep decrease in survivors below 50 m
532 that contrasted with the more gradual decrease of all individuals (Fig. 5). Copepod prey
533 concentrations were highest in the surface layer with maximum concentrations generally
534 between 0 to 35 m in 1995 and 0 to 65 m in 1998. Thus the majority of larvae in all cases
535 were at depths with high prey availability. There was a sharp decline in prey density
536 between 50 and 100 m coincident with the decreased abundance of surviving larvae (Fig.
537 5b,d,f,h).
538
539 Hatch distribution effect on survival and sources of mortality
540 The cross-initialization case demonstrated that both hatch locations and the
541 environment affected survival. The environment had the greatest influence on starvation,
542 with increased starvation in the 1995 environment, whereas advection losses depended
543 more strongly on hatch location, which were greater with the 1998 hatch locations (Table
544 8, Fig. 6). Larvae hatched in the 1995 February and March locations had greater percent
545 survival than those hatched in the 1998 locations under both environments. Cohorts
546 hatched in the 1995 locations experienced increased survival when in the 1998
547 environment (Table 8, Fig. 6a,b), while cohorts hatched in the 1998 locations experienced
548 a decrease in survival when in the 1995 environment (Table 8, Fig. 6c,d). With the
549 exception of the February cohorts in the 1995 environment, predation caused the plurality
550 of losses in all simulations (Table 8, Fig. 6).

551 Since hatch location and time influenced survival patterns, the fractions of
552 individuals hatched west or east of 67.5°W (midpoint of GB) that survived or were lost to
553 different sources of mortality were calculated for each cohort and year (Fig. 7). The
554 greatest differences in morality occurred in 1995. The dominant source of mortality of
555 larvae hatched in February 1995 was predation for those hatched west of 67.5°W (Fig.
556 7a) and starvation for those hatched to the east (Fig. 7b). The fate of larvae hatched to the
557 east in April 1995 (Fig. 7b) mimicked the pattern of all larvae (Fig. 6a). In contrast,
558 larvae hatched in April 1995 west of 67.5°W were predominantly lost to advection (Fig.
559 7a). Total advection losses were greater for cohorts hatched to the west of 67.5°W (66%
560 vs. 31%; Fig. 7a,b) in 1995 and to the east of 67.5°W in 1998 (35% vs. 15%; Fig. 7c,d).
561 As a result of all losses, the greatest fraction of survivors in 1995 were from
562 individuals hatched east of 67.5°W in the April cohort, followed by the eastern March
563 cohort, and then the western March cohort (Fig. 8 top left). The 1998 April cohort
564 hatched east of 67.5°W also contributed the most to the total number of survivors, but
565 was followed by the western April and the eastern March cohorts (Fig. 8 top right). Of all
566 the larvae in 1995, roughly 90% of those hatched and those that survived were hatched
567 east of 67.5°W (Fig. 8 bottom left). A greater fraction of larvae hatched on the western
568 side of the bank in 1998 (Fig. 8 bottom right). In both years, larvae hatched to the west
569 contributed more to survivors than to the total numbers hatched. In 1995 6.3% hatched to
570 the west, but 11.1% of survivors came from the west, with particular increases in the
571 February and March cohorts (Fig. 8 left). The amount hatched to the west of 67.5°W in
572 1998 was 27% of all larvae hatched and 34% of the survivors, mainly due to the April
573 cohort (Fig. 8 right).

574

575 Survival in the alternate hypotheses simulations

576 The fraction of individuals that survived out of those that hatched was greater in
577 1998 than 1995 for all cases (Fig. 9a). Temperature-dependent predation with a base
578 temperature of 5.5°C (TP5) resulted in the lowest survival per hatch in both years, while
579 DVM and temperature-dependent predation with a base temperature of 6.5°C (TP6) also
580 decreased survival from the reference for both years (Fig. 9a). Spatially-dependent
581 predation with increased rates on the crest and decreased rates on the flanks (CP) resulted
582 in the highest survival in both years, while increased flank predation (FP) also increased
583 survival rates (Fig. 9a). Though this seems counterintuitive, there was an asymmetry in
584 the losses to predation, advection, and starvation in these two cases such that the number
585 of survivors from reduced predation losses (CP; Fig. 10b) and reduced advection and
586 starvation losses (FP; Fig. 10a,c) outweighed the increased losses from the other
587 mortality sources in those simulations. Surprisingly, both increasing (95P+) and
588 decreasing (95P-) the total predation by 10% resulted in a greater number of survivors in
589 1995 (Fig. 9a). Again this was the result of an asymmetry in mortality where the
590 increased losses to predation and advection with 95P+ (Fig. 10a,c) were
591 overcompensated by decreased starvation (Fig. 10b). 1998 produced the expected
592 response of a 10% predation reduction (95P+) improving survival and a 10% increase
593 (95P-) lessening it (Fig 9a). In addition to the increases and decreases mentioned above,
594 the opposite environment (O) enhanced survival in 1995 but reduced it in 1998, which
595 also experienced survival decreases with the low prey (L) case (Fig. 9a).

596 The greater survival per hatch of all 1998 cases resulted in a ratio of survivors per
597 hatch in 1998 to 1995 greater than one (Fig. 9b). Mountain and Kane (2010) calculated
598 the number of recruits per hatched larva for the GLOBEC GB years. Comparing the
599 number of recruits per hatch in 1998 to 1995 yields a ratio of 1.17 (dashed line in Fig.
600 9b). The opposite environment simulation (O) produced the survivor per hatch ratio
601 (1.24) most similar to the recruits per hatch ratio of Mountain and Kane (2010). Of the
602 cases that simulated processes that could have realistically affected those years, the next
603 closest ratio of 1.32 occurred with interannually-varying predation that was greater in
604 1995 (95P+; Fig. 9b). Other comparable ratios were a result of reduced predation in 1995
605 (95P-), and spatially-varying flank predation (FP; Fig. 9b). All simulations lowered the
606 ratio below that of the reference case (2.45), which was most dissimilar from the
607 Mountain and Kane ratio (Fig. 9b).
608
609 The effect of alternate hypotheses on the sources of mortality
610 The fraction of larvae lost to advection was low compared to other mortality
611 sources, with greater loss in 1998 than 1995 for all cases (Fig. 10a). DVM, CP, and 95P+
612 increased advection losses in both years, with 95P- additionally increasing advection
613 losses in 1995 (Fig. 10a). Alternatively, FP, TP6, and TP5 lessened advective losses in
614 both years, with 95P- and L also reducing advective loss in 1998 (Fig. 10a). As noted
615 previously, 1995 hatch locations in the opposite environment suffered lower advection
616 losses, while 1998 hatch locations underwent the reverse effect (Fig. 10a). Percentages of
617 hatched larvae lost to predation were greater in 1995 than 1998 for all cases (Fig. 10b).
618 Starvation mortality in 1995 exceeded that in 1998 for 6 of the 10 cases. The 1995

619 cohorts suffered fewer starvation losses with the O, FP, 95P+, and L simulations (Fig.
620 10c). For both years, FP resulted in the greatest predation losses while CP led to the least
621 (Fig. 10b). These cases had the contrasting effect on starvation losses, the most from CP
622 and the least from FP (Fig. 10c). In all cases and years, the plurality of larvae (>0.4) were
623 lost to predation (Fig. 10).
624
625 Changes in cohort contribution from the reference
626 In 1995, the percent of total survivors from the February cohort was low across all
627 simulations. The contribution of this cohort was increased from the reference case by all
628 cases except DVM and CP (Fig. 11a). The results of the February 1998 cohort were
629 similar, except that O reduced the contribution and CP increased it (Fig. 11d). The
630 contributions of the March and April cohorts to all the surviving larvae in 1995 and 1998
631 tended to vary reciprocally (Fig. 11b,c,e,f). In 1995, all cases increased the contribution
632 of the March cohort and diminished that of the April cohort (Fig. 11b,c). In 1998, the CP,
633 FP, 95P+, TP6, and TP5 cases all increased the contribution of the March cohort and
634 decreased that of the April cohort (Fig. 11e,f). The variations in the contribution to
635 survivors by the different cohorts were smaller in 1998 with the largest changes occurring
636 for the 1995 March and April cohorts.
637
638 Growth rate
639 In comparison to 1995, the 1998 simulations had survivors with faster mean
640 specific growth rates (d^{-1}) from hatch until survival to 12 mm in all cases (Fig. 12).
641 Relative to the reference, 1995 growth rates were amplified by all cases except TP6 and

642 TP5 (Fig. 12). Both of these cases reduced growth rates in 1998, with the addition of
643 cases O, DVM, 95P-, and L (Fig. 12). In the O, DVM, and L simulations, the fraction of
644 larvae in 1998 lost to starvation was higher than the reference case (Fig. 10c), suggesting
645 that poor feeding gave rise to slower growth rates. Despite experiencing lower prey
646 concentrations than the reference with the O and L cases, growth rates of the 1998
647 simulations still exceeded those of 1995. With the exception of the February cohort, L
648 prey densities were greater than those experienced in 1995, even though they were
649 lowered to be comparable (Table 7). Mean prey availability was less for 1998 compared
650 to 1995 in the O case, thus the higher mean growth rates of 1998 must be accounted for
651 by spatially-dependent differences of the larvae with 1998 hatch locations, perhaps in
652 predation selecting for faster growth rates. Larvae in the 95P- case had a deeper weighted
653 mean depth than the reference case, thus lower temperatures, irradiance, and prey
654 densities could have reduced growth rates.
655
656
657
658
659
660
661
662
663
664

DISCUSSION

Coupled biological-physical modeling simulations revealed disparities in the processes occurring during the larval period of haddock on Georges Bank between the years of differing recruitment, 1995 and 1998. The overall model results suggest that increased initial numbers of hatched larvae and higher food availability (which reduced starvation and predation) in 1998 contributed to its larger year-class.

Vertical behavior

Diel vertical migration (DVM) of larvae greater than 9 mm reduced survival per hatch in both years and the mean growth rate in 1998. In general, lower survival stemmed from increased advection in both years and starvation in 1998. The increased starvation and lower growth rates can be attributed to the greater proportions of larvae deeper in the water column where temperatures, prey densities, and light intensities were lower. By comparing all larvae to those that survived to 12 mm, regardless of vertical behavior, it can be seen that depths above 30 m benefitted the February cohort, likely from higher prey concentrations and more light for feeding. On the other hand, more survivors from the March and April cohorts were found deeper than the February survivors. These cohorts experienced higher depth-integrated prey concentrations compared to larvae hatched in February, so did not need to be as shallow in the water column. These cohorts benefitted from deeper depths where visual predation rates were reduced. Though these larvae survived by avoiding predation, their growth rates were lower in 1998 than if they had been shallower. Moreover, the 20 m nighttime depth could have been detrimental to all cohorts by increasing near-surface advection loss.

688 The vertical behavior used in the DVM simulation was an inadequate
689 representation for larval haddock on Georges Bank, as behavior should not decrease
690 survival. Observations of the vertical distribution of larval haddock and their prey
691 (Lough, 1984; Buckley & Lough, 1987; Lough & Potter, 1993) suggest that the larvae
692 have a prey-seeking vertical migration behavior. Conversely, larvae may have a preferred
693 depth unrelated to prey that prevents advection off the bank. The modeling results of
694 Werner *et al.* (1993, 1996) suggest that larvae must stay below 30 m to remain on the
695 bank, despite observations of larvae above this depth. Regardless of whether the vertical
696 behavior of larval haddock is aimed at finding prey, avoiding predation, or avoiding
697 advection, the mechanism governing the behavior has not been determined and is an
698 important area for future research.
699
700 *Hatch date of survivors*
701 Lapolla and Buckley (2005) back-calculated the hatch date of young-of-year juvenile
702 haddock and found that the hatch date frequency of the surviving juveniles peaked
703 between February and mid-March, with 1998 having a significantly later peak hatch date
704 than 1995. More larvae hatched in April and May of 1998 survived than the 1995-1999
705 average, but the highest survival was still from the early hatch dates (Lapolla & Buckley,
706 2005). Mountain *et al.* (2008) also found that the peak contribution of each cohort
707 occurred in March of 1995 and 1998 by back calculating hatch dates from larval
708 abundances and estimated mortality rates. The contributions to total survival from the
709 modeled February and March cohorts were low in the reference simulation, but both
710 temperature-dependent predation cases increased their contributions in both years.

711 The temperature-dependent predation rate was used to test the hypothesis that
712 early-hatched haddock are the dominant survivors because they reach an invulnerable
713 size before their predators become abundant (Lapolla & Buckley, 2005; Buckley &
714 Durbin, 2006; Buckley *et al.*, 2010). Temperature-dependent predation increased the
715 February and March cohort contributions while decreasing that of the April cohort even
716 though it failed to increase the fraction of survivors above that from April. Part of the
717 discrepancy between our results and theirs could be that we measured survival at the end
718 of the larval period rather than during the juvenile stage. Nevertheless, a different
719 parameterization of temperature-dependent predation may result in cohort contributions
720 that agree better with observations of the mean hatch date of survivors. The predation rate
721 could be further improved by representing temperature-related increases in consumption
722 rates and seasonal increases in predator abundances.
723 Observations from 1976-1987 (Lough *et al.*, 2006) and 1995-1999 (Mountain *et*
724 *al.*, 2008) show peak haddock spawning between March and April. Evolutionarily, the
725 peak in spawning and subsequent hatching should be timed to result in the highest
726 survival of eggs and larvae. During the 1976-1987 period, the large and moderate year-
727 classes of haddock were spawned in April and benefitted from high hatching rates, high
728 physical retention, high prey concentrations in May, and a late seasonal temperature-
729 dependent growth optimum (Lough *et al.*, 2006). In contrast, observations from the 1995-
730 1999 GLOBEC GB study period demonstrate a mismatch between the time of peak
731 hatching and time when most survivors hatched (Lapolla & Buckley, 2005; Mountain *et*
732 *al.*, 2008). For example, 1998 peak spawning occurred between February and March

733 (days 45-85) followed by peak hatching in April (day 115), but the peak hatch time of
734 survivors was in early March (day 65; Mountain *et al.*, 2008).
735 Following the seasonal predation hypothesis (Lapolla & Buckley, 2005; Buckley
736 & Durbin, 2006; Buckley *et al.*, 2010), there could have been a decadal shift in the
737 predator community on Georges Bank that resulted in higher predation rates in April and
738 May for 1995-1999 compared to 1976-1987 and thus the earlier hatch dates of survivors.
739 This shift in the predator community could be related to the increased zooplankton
740 abundance on Georges Bank that occurred in the 1990s (Mountain & Kane, 2010).
741 Similarly, bottom-up biological processes in 1995-1999 could have caused prey
742 concentrations in February and March that were high enough to support growth to a size
743 invulnerable to predators. A potential mechanism responsible for this hypothesis is
744 increased stratification from the input of low salinity water into the Gulf of Maine and
745 Georges Bank from the Arctic, which could produce an earlier spring bloom and earlier
746 development of larval haddock prey populations (Ji *et al.*, 2008). Regardless of the cause
747 of the mismatch in peak hatching time of all eggs and just those that survived, if this state
748 persists, one might expect the adult haddock population to shift its peak spawning time to
749 coincide with the ideal conditions.
750 Alternatively, the time of peak spawning may be controlled by the age structure of
751 the adult population. Age-2 females of the North Sea haddock population spawned 27-36
752 days later than older females in 1994, 1996, and 1999 (Wright & Gibb, 2005). Similar to
753 the 1995-1999 observations from the Georges Bank population, the timing of peak spawn
754 date of surviving North Sea juveniles was earlier than the peak in egg production in 1996
755 and 1999 (Wright & Gibb, 2005). Wright and Gibb (2005) suggested that the negative

selection on late spawning dates was the result of less viable eggs and larvae produced by the age-2 females. This hypothesis is supported by the fact that older haddock females produce larger eggs (Hislop 1988) from which larger larvae hatch (Rideout *et al.*, 2005). Larger larvae have more advanced morphological characteristics that could confer survival advantages during the first few days after hatch (Rideout *et al.*, 2005). In addition, haddock are batch spawners and egg size decreases with each batch spawned (Rideout *et al.*, 2005). Thus, the early hatch date of surviving haddock in the Georges Bank population could be the product of high mortality of the many small eggs spawned late in the year as last batches and/or from young females, and it merits further study.

Advection

Larvae followed the general clockwise circulation pattern of Georges Bank. Advection only losses of 3-24% of a cohort were congruent with Georges Bank studies of modeled retention rates between 20 and 65% (Lewis *et al.*, 2001; Lough *et al.*, 2006), and residence times of <10 d to 70 d estimated from drouged drifters (Colton & Anderson, 1983) and a particle-tracking model (Page *et al.*, 1999). The 1998 egg hatching patterns resulted in larvae developing all over the bank, while the 1995 cohorts were absent from the Northern Flank. Advective losses were greater in 1998 despite this year having lower off-bank wind stress (Mountain *et al.*, 2008). In general, these higher losses in the 1998 model runs were due to hatch locations that made larvae more susceptible to advective loss, and not the result of between-year differences in the physical circulation. If advection had been the only source of mortality for larvae, haddock in 1995 would have had higher survival per hatch than in 1998.

779 Chase (1955) examined haddock recruitment from 1928 to 1951 in relation to
780 wind-driven advection on Georges Bank. Weighted "damage units" to recruitment were
781 assigned to the number of days with a continuous pressure difference between Nantucket,
782 Massachusetts and Yarmouth, Nova Scotia, a proxy for the component of geostrophic
783 wind that drives current perpendicular to the southern edge of Georges Bank. Chase
784 (1955) found a significant correlation between year-class strength and the damage total
785 from spawning (defined as when the rate of change of surface temperature lessens) until
786 May 1. Similarly, Mountain *et al.* (2008) found a strong correlation between recruitment
787 of haddock during the GLOBEC GB period of 1995-1999 and the estimated number of
788 hatched eggs, with interannual variability in egg mortality related to wind-driven
789 transport off the Southern Flank of Georges Bank. The correlation between recruitment
790 and the number of larvae reaching 15 dph was almost as high as the recruitment
791 correlation with egg hatching, however, there was no relationship between larval
792 mortality rates and wind-driven transport (Mountain *et al.*, 2008). Combined, their results
793 and ours suggest that the influence of advection losses on recruitment spanned the entire
794 early life period (spawn to May 1) for 1928-1951, and shifted to only during the egg
795 stage for 1995-1999.
796 As mentioned in the *Methods* section, advection past the 200 m isobath was a
797 proxy for starvation from leaving the rich prey environment of Georges Bank, heavy
798 predation off the slope of the bank, and the inability to find suitable juvenile settlement
799 habitat. Alternatively, each of these processes could be modeled. Super-individuals and
800 individuals were followed for the entire duration of the simulation, such that information
801 on starvation, predation, and location were available after a larva left the region denoted

802 by the 200 m isobath as long as it remained in the model domain. Many of these
803 individuals starved and/or were eaten after advective loss in the model simulations.
804 Though potential prey would be advected off the bank in the same mass of water that
805 contained the larvae being advected, starvation would occur from spatial and temporal
806 mismatch of the larvae and prey. If larvae swam out of the layer of water that was
807 advected, they would immediately experience the lower prey densities off the continental
808 slope. Also, prey concentration would decrease as both the prey and their resources were
809 diluted in the deep-ocean environment and as the prey were eaten by many of the same
810 slope-water predators that would consume the larval fish. As with all predation, it is
811 difficult to determine how to parameterize the off-bank predation rates to simulate the
812 losses to mesopelagic fish and other predators. Finally, it is possible for larvae to be
813 advected back onto the bank before experiencing either starvation or predation, thus true
814 advective loss should be determined from individuals that are not near the favorable
815 pebble-gravel settlement habitats on Georges Bank (Lough *et al.*, 1989) at the time of the
816 demersal transition. As this transition from a pelagic to demersal lifestyle happens during
817 the juvenile stage, it could not be simulated in the present study because the physiological
818 and behavioral models do not hold for juvenile haddock.
819
820 *Predation*
821 Predation accounted for the most losses in all simulations. Percent loss to predation
822 increased with hatch date, which is contrary to the hypothesis that larvae with faster
823 growth rates (March 1995, April 1998) would be exposed to predation for less. However,
824 like the larval fish, the visual predators benefited from longer photoperiods and greater

825 light intensities later in the season, which increased predation rates. Furthermore,
826 starvation losses decreased with hatch date, which left more live larvae available for
827 predators to eat. Total predation losses were higher in 1995, suggesting that the smaller,
828 slower growing larvae were more susceptible to predation. This conclusion is further
829 supported by the systematic addition of mortality sources. When predation was added as
830 a source in addition to advection and starvation, it claimed a greater fraction of larvae that
831 would have eventually starved.

832 Altering the predation rate was the only way to increase the contributions of early
833 hatch dates to the surviving juveniles as observed. All temperature-dependent predation
834 and some spatially dependent predation cases increased the contributions of the February
835 and March cohorts and decreased those of April. It can be inferred that a predation rate
836 that increased with temperature most likely contributed to the observations of early hatch
837 dates of survivors, while a spatial predation component may have also played a role.

838 There are many types of potential invertebrate predators of fish larvae such as
839 chaetognaths (Kuhlmann, 1977), copepods (e.g. *Euchaeta norvegica*; Bailey, 1984; Yen,
840 1987), amphipods (e.g. *Parathemisto* spp.; Sheader & Evans, 1975; Yamashita *et al.*,
841 1985), mysids (Bailey, 1984), decapod shrimps (e.g. *Crangon septemspinosa*; Wilcox &
842 Jeffries, 1974), euphausiids (Bailey, 1984), hydroids (Madin *et al.*, 1996), medusae
843 (Bailey, 1984; Purcell, 1985), and siphonophores (Purcell, 1985), as well as vertebrate
844 predators like Atlantic herring (*Clupea harengus*) and mackerel (*Scomber scombrus*;
845 Garrison *et al.*, 2000). Most of these predators are opportunistic such that the prey items
846 found in their guts reflect the natural abundances of the plankton. Since fish larvae are
847 rather dilute (0-2.5 m^{-3}; Lough, 1984), it is doubtful that they make up a significant

848 portion of any opportunistic predator's diet. Even though predation of fish larvae may be
849 incidental, there may be considerable loss of larvae if predator abundances and
850 consumption rates are high.
851 Chaetognaths are probably not significant predators on larval haddock since they
852 can only eat larvae within a narrow time period after hatch (4 dph) because of size
853 limitations (Kuhlmann, 1977). Similarly, the copepod *E. norvegica* cannot consume
854 larvae >7 mm (Bailey, 1984). In addition, its consumption rate of larval fish is low in
855 comparison to medusae and euphausiids (Bailey, 1984) and it is the least abundant of all
856 potential invertebrate predators on Georges Bank (Sullivan & Meise, 1996), thus
857 negating it as a dominant predator. Though the filtering rates of mackerel could lead to
858 high predation losses, their lack of spatial and temporal overlap on Georges Bank with
859 haddock larvae discounts them as important predators (Garrison *et al.*, 2000). Suspended
860 hydroid colonies can be another significant predator of fish larvae on the crest of Georges
861 Bank (Madin *et al.*, 1996), unfortunately, these and other gelatinous predators are
862 difficult to sample.
863 Consequently, we examined the potentially significant predators for which there
864 was abundance data from the GLOBEC GB cruises (amphipods, mysids, *C.*
865 *septemspinosa*, euphausiids, siphonophores, and herring). We assessed these data for
866 interannual differences that could substantiate the survivor per hatch ratios of the
867 simulations with interannually varying predation and higher flank predation, and for
868 seasonal differences that increased the contributions of the February and March cohorts
869 in several simulations. Herring stock estimates indicate that the population was greater in
870 1998 (DFO, 2003), while some invertebrate predators were more abundant in 1995 (Fig.

13). Neither the presence of euphausiids (p=0.71), mysids (p=0.50), and *C. septemspinosa* (p=1.00), nor their abundance when found (p=0.13, p=0.38, p=0.81, respectively) was significantly different in 1995 and 1998. In contrast, there was a greater chance of collecting siphonophores (p<0.01) and hyperiid amphipods (p=0.02) in 1995, and the abundances of these predators were significantly higher in 1995 (p<0.01 and p=0, respectively; Fig. 13).

It is very possible that the greater abundances of siphonophores and hyperiid amphipods in 1995 compared to 1998 resulted in greater predation rates in 1995 and the observed differences in survival rate. Unlike the other invertebrate predators that eat fish larvae incidentally, larvae can comprise 90-100% of the diets of cystonect siphonophores and are frequently consumed by physonect siphonores (Purcell, 1981; 1985). The many gastrozooids of siphonophores allow them to ingest more than one larva at a time (Purcell, 1985). Hyperiid amphipods can also have a detrimental effect on larval fish populations depending on densities of predator and prey, and on their spatial and temporal overlap. For example, predation by the hyperiid amphipod *Parathemisto japonica* resulted in daily predation losses up to 45.2% of sand-eel larvae (Yamashita *et al.*, 1985).

The importance of siphonophores and hyperiid amphipods as predators on haddock larvae is further supported by their lowest abundances occurring in March (Fig. 13), which could lead to an increase in the contribution of larvae hatched during this month as observed (Lapolla & Buckley, 2005; Mountain *et al.*, 2008). The climatological distributions of siphonophores and hyperiids indicate greater abundances outside the 60 m isobath (Sullivan & Meise, 1996), which lends credence to model

894 predictions of a survival per hatch ratio similar to the Mountain and Kane (2010) ratio
895 and increased contributions of the February and March cohorts with the higher flank
896 predation simulation.

897 Conversely, mysids and *C. septemspinosa* are more abundant on the crest region
898 inside 60m (Davis, 1987; Sullivan & Meise, 1996). The mysid abundance was also
899 lowest in March (Fig. 13). An increase in crest predation rates raised early cohort
900 contributions for 3 of the 4 February and March cohorts, but not as much as increased
901 flank predation rates. Similarly, high crest predation reduced the survivor per hatch ratio,
902 but the ratio of the high flank predation case was more similar to the Mountain & Kane
903 (2010) ratio. Thus, the fact that mysids and *C. septemspinosa* were not significantly more
904 abundant in 1995 might be irrelevant if predation in this region is not important in driving
905 interannual variability in larval survival. Additionally, the warm water intrusions in 1995
906 could have advected slope water predators onto Georges Bank (Brown *et al.*, 2005),
907 thereby increasing overall predation rates, as well as rates on the flank.

908 Neither the interannual nor the spatial pattern in predation rates on Georges Bank
909 is fully resolved, and neither can be used to reject or accept the simulations of increased
910 predation rates in 1995, decreased predation in 1995, and increased flank predation that
911 each produced modeled survival per hatch ratios approximating the recruits per hatch
912 ratio of Mountain and Kane (2010), and in the case of flank predation, enhanced the
913 contribution of the February and March cohort contributions to survivors. However, the
914 high larval fish ingestion rates and the seasonal abundance pattern of mysids,
915 siphonophores, and hyperiid amphipods suggest these taxa are important predators of
916 larval haddock. This analysis was a small effort to understand the spatially and

917 temporally dependent predation rates on Georges Bank. Further work is required in the
918 form of horizontal and vertical distributions of predators and consumption rates on larval
919 fish since predation mortality is the most uncertain component in larval fish models, and
920 one that can have substantial effects.
921
922 *Starvation and growth*
923 Though starvation was not responsible for the largest fraction of larval mortality, food-
924 limitation determined the interannual variability in survival of haddock larvae in 1995
925 and 1998. When advection was considered the only source of loss, survival per hatch was
926 greater in 1995 than 1998. By adding starvation as a mortality source, percent survival
927 became greater in 1998 compared to 1995. The high survival rates of 1998 ought to have
928 been a direct result of higher growth rates and lower starvation losses from the greater
929 *Pseudocalanus* spp. concentrations. Buckley *et al.* (2006) report very low incidence of
930 starvation in 5-12 mm larvae of haddock, however direct starvation of larvae is difficult
931 to observe since malnourished larvae are smaller and have higher predation rates. This
932 likely explains why modeled losses to predation were higher in 1995 and lower in 1998.
933 Not only did fewer larvae in 1998 starve to death, but faster growth from higher prey in
934 1998 could have led to larvae that were vulnerable to predation for less time (Davis *et al.*,
935 1991). Slow growing larvae in 1995 would have been exposed to predators for a longer
936 amount of time, and would have experienced higher predation rates by being smaller at a
937 given time and less able to avoid capture.
938 Starvation decreased with hatch date because as the season progressed, both
939 photoperiod and copepod prey concentrations increased, allowing for the consumption of

940 more biomass. These seasonal increases were somewhat reflected in the modeled growth
941 rates and mean times to 12 mm. The growth rate of the 1998 April cohort was high from
942 the dramatic increase in the copepod population later in the season such that food was not
943 limiting. The higher growth rates later in the season may have skewed the mean growth
944 rates of all cohorts and mitigated the effect of prey availability on total survivorship.
945 The growth rate of haddock larvae is strongly correlated with the *Pseudocalanus*
946 spp. biomass with a Michaelis-Menten type response (Buckley & Durbin, 2006). The
947 modeled weighted mean growth rates of surviving 5-7 mm larvae were much lower than
948 the curve derived from RNA:DNA measurements (Buckley and Durbin 2006; Fig. 14a),
949 potentially indicating a higher half-saturation biomass concentration, lower maximum
950 growth rate, and/or a non-zero concentration needed for positive growth. The
951 disagreement between the 5-7 mm model results and the empirical curve could be
952 accounted for by differing temperatures that larvae were exposed to in the model and in
953 1992-1994 when Buckley and Durbin (2006) sampled. If temperature was not the cause,
954 then either the model did not correctly represent some aspect of the growth of 5-7 mm
955 larvae, or the model failed to kill slower growing larvae that died in the ocean and were
956 not sampled by Buckley and Durbin (2006). Potential sources of error in the growth
957 model include modeled *Pseudocalanus* spp. concentrations without sufficient resolution
958 in the vertical dimension, possibly by not representing micropatchiness (Davis *et al.*,
959 1991), and mischaracterization of consumption rates from aggregating the copepod stages
960 and using mean parameter values across the stages. Alternatively, the starvation threshold
961 in the model may be too low, which could account for the divergent growth rates if
962 slower growing larvae die in the ocean but not in the model. Despite the discrepancy for

963 5-7 mm larvae, the simulated 7-12 mm survivors had growth rates that correspond well
964 with the maximum growth rate calculated by Buckley and Durbin (2006; Fig. 14b). Since
965 these growth rates were at the maximum, it must have been growth and starvation during
966 the early larval period (hatch to 7 mm) that was most important to interannual variability
967 in survival.
968
969 *Survival*
970 The percent of hatched larvae that survived was greater in 1998, in agreement with
971 estimates of percent of hatched larvae that survived to 15 dph (Mountain *et al.*, 2008) and
972 that recruited (Mountain & Kane, 2010). The overestimation of the modeled survivor per
973 hatch ratio compared to the recruit per hatch ratio of Mountain and Kane (2010) could be
974 for several reasons. One, the modeled *Pseudocalanus* spp. prey concentrations do not
975 capture important spatial and/or temporal differences between the two years. This source
976 of error could be examined with a more detailed copepod population model. Two,
977 inclusion of copepod eggs and other copepod species as prey could reduce starvation in
978 1995 and compensate for the difference between the two ratios. Though the four
979 dominant prey taxa were more abundant in 1998 than 1995 (Buckley & Durbin, 2006),
980 the gut contents of haddock larvae indicated positive feeding preferences for other
981 copepod species in 1995; unfortunately preferences from 1998 were unavailable
982 (Broughton & Lough, 2010). Three, the magnitude of the predation rate, its relationship
983 with larval fish size, and its variability vertically, horizontally, seasonally, and/or
984 interannually are uncertain. The base predation rate was parameterized as best as possible
985 to agree with mortality estimates for larval fish, and the inverse relationship with larval

size agrees with calculations of decreased mortality with increasing larval age from the GLOBEC GB study period (Mountain *et al.*, 2008). Fourth and finally, the processes responsible for the discrepancy between the modeled survivor per hatch ratio and the recruit per hatch ratio could occur during the juvenile stage, which was not included in this model.

The higher total numbers of surviving larvae in the reference simulations of 1998 compared to 1995 appear to be related to the greater number of larvae hatched in 1998. Since the number surviving was only a small percentage of the initial number of larvae, changes in predation, advection, and growth were expected to be important causes of changes in numbers of surviving larvae between years. However, the initial abundance and distribution of hatched larvae was critically important, as can clearly be seen in the run with opposite environment, i.e., the larvae hatched at the 1998 locations but subjected to the 1995 environmental conditions still had a greater number of survivors even though percent survival was lower. The largest proportion of larvae that hatched and that survived were hatched east of 67.5°W in both 1995 and 1998. However, larvae that originated west of 67.5°W composed a greater fraction of the total survivors than the total number hatched. Depending on temperature, the egg stage ranges from 10 to 20 d (mean 16 d; Page & Frank, 1989). Based on the circulation of Georges Bank, it is likely that the larvae that hatched west of 67.5°W were also spawned on that side of the bank, and the modeled proportions of 6% and 27% of larvae hatched in 1995 and 1998 compare favorably with observed proportions of 4% and 30% of the eggs spawned in those locations in those years (Mountain *et al.*, 2008). Though spawning predominantly occurs on the Northeast Peak (NEP), spawning on western Georges Bank can contribute

1009 survivors in the winter when advective loss from the surface waters of the NEP is highest
1010 (Lough *et al.*, 2006). Notably, hatching success, which contributed to the higher survival
1011 in 1998 simulations, is significantly correlated to the fraction of eggs spawned west of
1012 67.5°W, and not to the total number of eggs spawned (Mountain *et al.*, 2008).
1013
1014 *Conclusions*
1015 From the model results, we conclude that the survival of larval haddock on Georges Bank
1016 is dominated by food-limitation, particularly from hatch to 7 mm, with both starvation
1017 and slower growth leading to higher predation and longer exposure to predation acting as
1018 important sources of mortality. Both starvation and predation losses were greater in
1019 simulations of larval haddock in 1995, thus it must have been the higher prey
1020 concentrations in 1998 that resulted in observations of higher survival and recruitment
1021 per hatched larvae in 1998 compared to 1995 (Mountain *et al.*, 2008; Mountain & Kane,
1022 2010). Temperature-dependent predation rates resulted in cohort contributions that better
1023 agreed with observations of the mean hatch date of survivors, further supporting the
1024 hypothesis that seasonal increases in predation rate favor survival of larvae from earlier
1025 hatch dates (Lapolla & Buckley, 2005; Mountain *et al.*, 2008). The importance of
1026 advection during the larval period was negated by the fact that modeled advective losses
1027 were small in general, and higher in 1998 despite lower wind stress that year, due to
1028 hatch location. This conclusion is corroborated by Mountain *et al.* (2008), who did not
1029 find a relationship between modeled wind-driven transport and early larval mortality
1030 rates.

In addition to higher prey concentrations leading to increased growth rates and decreased starvation, the greater total number of survivors in 1998 was related to the greater number of eggs that hatched in that year. The better hatching success of 1998 was a result of weaker southeastern wind stress and a larger proportion of eggs spawned on the western part of Georges Bank (Mountain *et al.*, 2008). The number of haddock eggs spawned is not significantly correlated to recruitment, whereas egg hatching and larval survival are correlated to recruitment (Mountain *et al.*, 2008). Mountain *et al.* (2008) found that the contributions of egg and larval mortalities to overall haddock survivorship were comparable. In light of their results and the modeling work presented here, we conclude that interannual differences in haddock recruitment during the 1995-1999 GLOBEC GB study period were dominated by advection during the embryonic period and food-limitation during the larval stage. Our results suggest that food-limitation and its related losses to starvation and predation may be responsible for interannual variability in recruitment and larval survival outside of the years studied. Further research is needed to assess whether these patterns hold for other years.

ACKNOWLEDGEMENTS

Financial support was provided by a WHOI Watson Fellowship, a WHOI Coastal Ocean Institute Student Research Proposal Award, and GLOBEC grants NA17RJ1223 (NOAA) and OCE0815838 (NSF). We would like to thank D.G. Mountain for providing the egg hatching rate data, R.G. Lough for discussions on haddock larvae and predators, and A. Solow for statistical assistance. This manuscript benefitted from the comments of K.A.

Rose and 2 anonymous reviewers. This is contribution number XXXX of the GLOBEC program.

REFERENCES

Aksnes, D.L., and Giske, J. (1993) A theoretical model of aquatic visual feeding. *Ecol. Model.* **67:** 233-250.

Aksnes, D.L., and Utne, A.C.W. (1997) A revised model of visual range in fish. *Sarsia* **82:** 137-147.

Bailey, K.M. (1984) Comparison of laboratory rates of predation on five species of marine fish larvae by three planktonic invertebrates: effects of larval size on vulnerability. *Mar. Biol.* **79:** 303-309.

Bailey, K.M., and Houde, E.D. (1989) Predation on eggs and larvae of marine fishes and the recruitment problem. *Adv. Mar. Biol.* **25:** 1-83.

Brodziak, J., and Traver, M. (2006) Status of fishery resources off the Northeastern US: haddock. URL: http://www.nefsc.noaa.gov/sos/spsyn/pg/haddock/. [Last accessed January 2013]

Broughton, E.A., and Lough, R.G. (2010) General trends and interannual variability in prey selection by larval cod and haddock from the Southern Flank of Georges Bank, May 1993-1999. *NOAA Tech Memo NMFS-NE* **217:** 38pp.

Brown, H., Bollens, S.M., Madin, L.P., and Horgan, E.F. (2005) Effects of warm water intrusions on populations of macrozooplankton on Georges Bank, Northwest Atlantic. *Cont. Shelf Res.* **25:**143-156.

1076 Buckley, L.J., and Durbin, E.G. (2006) Seasonal and inter-annual trends in the
1077 zooplankton prey and growth rate of Atlantic cod (*Gadus morhua*) and haddock
1078 (*Melanogrammus aeglefinus*) larvae on Georges Bank. *Deep-Sea Res. II* **53:**
1079 2758-2770.
1080 Buckley, L.J., and Lough, R.G. (1987) Recent growth, biochemical composition, and
1081 prey field of larval haddock (*Melanogrammus aeglefinus*) and Atlantic cod
1082 (*Gadus morhua*) on Georges Bank. *Deep-Sea Res. II* **44:** 14-25.
1083 Buckley, L.J., Caldarone, E.M., and Lough, R.G. (2004) Optimum temperature and food-
1084 limited growth of larval Atlantic cod (*Gadus morhua*) and haddock
1085 (*Melanogrammus aeglefinus*) on Georges Bank. *Fish. Oceanogr.* **13:** 134-140.
1086 Buckley, L.J., Caldarone, E.M., Lough, R.G., and St. Onge-Burns, J.M. (2006)
1087 Ontogenetic and seasonal trends in recent growth rates of Atlantic cod and
1088 haddock larvae on Georges Bank: effects of photoperiod and temperature. *Mar.*
1089 *Ecol. Prog. Ser.* **325:** 205-226.
1090 Buckley, L.J., Lough, R.G., and Mountain, D. (2010) Seasonal trends in mortality and
1091 growth of cod and haddock larvae result in an optimal window for survival. *Mar.*
1092 *Ecol. Prog. Ser.* **405:** 57-69.
1093 Butman, B., and Beardsley, R.C. (1987) Long-term observations on the southern flank of
1094 Georges Bank. Part I: A description of the seasonal cycle of currents, temperature,
1095 stratification, and winds stress. *J. Phys. Oceanogr.* **17:** 367-384.
1096 Butman, B., Beardsley, R.C., Magnell, B., Frye, D., Vermersch, J.A., Schlitz, R.,
1097 Limeburner, R., Wright, W.R., and Noble, M.A. (1982) Recent observations of
1098 the mean circulation on Georges Bank. *J. Phys. Oceanogr.* **12:** 569-591.

1099 Caparroy, P., Thygesen, U.H., and Visser, A.W. (2000) Modelling the attack success of
1100 planktonic predators: patterns and mechanisms of prey selectivity. *J. Plank. Res.*
1101 **22:** 1871-1900.
1102 Chase, J. (1955) Winds and temperature in relation to the brood-strength of Georges
1103 Bank haddock. *J. Cons. Int. Explor. Mer* **21:**17-24.
1104 Chen, C. (1992) Variability of currents in Great South Channel and over Georges Bank:
1105 observation and modeling. Ph.D. thesis, Massachusetts Institute of Technology,
1106 283pp.
1107 Chen, C., Liu, H., and Beardsley, R.C. (2003) An unstructured, finite-volume, three
1108 dimensional, primitive equation oceanography model: application to coastal
1109 oceanography and estuaries. *J. Atmos. Ocean Tech.* **20:** 159-186.
1110 Chen, C., Cowles, G., and Beardsley, R.C. (2006) An unstructured grid, finite-volume
1111 coastal ocean model: FVCOM User Manual, Second Edition. *SMAST/UMASSD*
1112 *Technical Report 06-0602:* 315pp.
1113 Churchill, J., Runge, J., and Chen, C. (2011) Processes controlling retention of spring
1114 spawned Atlantic cod (*Gadus morhua*) in the western Gulf of Maine and their
1115 relationship to an index of recruitment success. *Fish. Oceanogr.* **20:** 32-46.
1116 Colton, Jr., J.B., and Anderson, J.L. (1983) Residual drift and residence time of Georges
1117 Bank surface waters with reference to the distribution, transport, and survival of
1118 larval fishes. *NOAA Tech. Memo. NMFS-F/NEC* **24:** 54pp.
1119 Davis, C.S. (1984) Predatory control of copepod seasonal cycles on Georges Bank. *Mar.*
1120 *Biol.* **82:** 31-40.
1121 Davis, C.S. (1987) Zooplankton life cycles. In: *Georges Bank.* R.H. Backus and D.W.

1122 Bourne (eds) London: MIT Press, pp. 1-593.
1123 Davis, C.S., Flierl, G.R., Wiebe, P.H., and Franks, P.J.S. (1991) Micropatchiness,
1124 turbulence and recruitment in plankton. *J. Mar. Res.* **49**: 109–151.
1125 DFO (2003) Atlantic herring: Georges Bank, Nantucket Shoals, Gulf of Maine stock
1126 complex. Nova Scotia: Department of Fisheries and Oceans Science Stock Status
1127 Report 2003/028. 7pp.
1128 Fiksen, Ø., and MacKenzie, B.R. (2002) Process-based models of feeding and prey
1129 selection in larval fish. *Mar. Ecol. Prog. Ser.* **243:** 151-164.
1130 Fiksen, Ø., and Jørgensen, C. (2011) Model of optimal behaviour in fish larvae predicts
1131 that food availability determines survival, but not growth. *Mar. Ecol. Prog. Ser.*
1132 **432:** 207-219.
1133 Flierl, G.R., and Wroblewski, J.S. (1985) The possible influence of warm core Gulf
1134 Stream rings upon shelf water larval fish distributions. *Fish. Bull.* **83:** 313-330.
1135 Folkvord, A. (2005) Comparison of size-at-age of larval Atlantic cod (*Gadus morhua*)
1136 from different populations based on size- and temperature-dependent growth
1137 models. *Can. J. Fish. Aquat. Sci.* **62:** 1037-1052.
1138 Garrison, L.P., Michaels, W., Link, J.S., and Fogarty, M. (2000) Predation risk on larval
1139 gadids by pelagic fish in the Georges Bank ecosystem. I. Spatial overlap
1140 associated with hydrographic features. *Deep-Sea Res. II* **57:** 2455-2469.
1141 GLOBEC (1992) U.S. GLOBEC: Northwest Atlantic Implementation Plan. *GLOBEC*
1142 *Rep.* No **6:** 81pp.
1143 Heath, M.R., and Lough, R.G. (2007) A synthesis of large-scale patterns in the planktonic
1144 prey of larval and juvenile cod (*Gadus morhua*). *Fish. Oceanogr.* **16:** 169-185.

1145 Hislop, J.R.G. (1988) The influence of maternal length and age on the size and weight of
1146 the eggs and the relative fecundity of the haddock, *Melanogrammus aeglefinus*, in
1147 British waters. *J. Fish. Biol.* **32:** 923-930.
1148 Hjort, J. (1914) Fluctuations in the great fisheries of Northern Europe viewed in the light
1149 of biological research. *Rapp. P.-v. Réun. Cons. Int. Explor. Mer* **20:** 1-228.
1150 Houde, E.D. (1989) Comparative growth, mortality, and energetics of marine fish larvae:
1151 temperature and implied latitudinal effects. *Fish. Bull.* **87:** 471-495.
1152 Hu, Q., Davis, C.S., and Petrik, C.M. (2008) A simplified age-stage model for copepod
1153 population dynamics. *Mar. Ecol. Prog. Ser.* **360:** 179-187.
1154 Huret, M., Runge, J.A., Chen, C., Cowles, G., Xu, Q., and Pringle, J.M. (2007) Dispersal
1155 modeling of early life stages: sensitivity analysis with application to Atlantic cod
1156 in the western Gulf of Maine. *Mar. Ecol. Prog. Ser.* **347:** 261-274.
1157 Jennings, S., and Mackinson, S. (2003). Abundance-body mass relationships in size
1158 structured food webs. *Ecol. Lett.* **6:** 971-974.
1159 Ji, R., Ashjian, C., Campbell, R., Chen, C., Gao, G., Davis, C., Cowles, G., and
1160 Beardsley, R. (2012) Life history and biogeography of *Calanus* copepods in the
1161 Arctic Ocean: An individual-based modeling study. *Prog. Oceanogr*. **96:** 40-56.
1162 Ji, R., Davis, C.S., Chen, C., Townsend, D.W., Mountain, D.G., and Beardsley, R.C.
1163 (2008) Modeling the influence of low-salinity water inflow on winter-spring
1164 phytoplankton dynamics in the Nova Scotian Shelf-Gulf of Maine region. *J.*
1165 *Plank. Res.* **30:** 1399-1416.
1166 Ji, R., Davis, C.S., Chen, C., and Beardsley, R.C. (2009) Life history traits and

1167 spatiotemporal distributional patterns of copepod populations in the Gulf of
1168 Maine-Georges Bank region. *Mar. Ecol. Prog. Ser.* **384:** 187-205.
1169 Ji, R., Stegert, C., and Davis, C.S. (2012) Sensitivity of copepod populations to bottom
1170 up and top-down forcing: a modeling study in the Gulf of Maine region. *J. Plank.*
1171 *Res.* doi: 10.1093/plankt/fbs070.
1172 Jones, R. (1973) Density-dependent regulation of the numbers of cod and haddock. *Rapp.*
1173 *P.-v. Réun. Cons. Int. Explor. Mer* **164:** 119-127.
1174 Kane, J. (1984) The feeding habits of co-occurring cod and haddock larvae from Georges
1175 Bank. *Mar. Ecol. Prog. Ser.* **16:** 9-20.
1176 Kristiansen, T., Fiksen, Ø., and Folkvord, A. (2007) Modelling feeding, growth and
1177 habitat selection in larval cod (*Gadus morhua*): observations and model
1178 predictions in a macrocosm environment. *Deep-Sea Res. II* **64:** 136-151.
1179 Kristiansen, T., Jørgensen, C., Lough, R.G., Vikebø, F., and Fiksen, Ø. (2009) Modeling
1180 rule-based behavior: habitat selection and the growth-survival trade-off in larval
1181 cod. *Behav. Ecol.* **20:** 490-500.
1182 Kuhlmann, D. (1977) Laboratory studies on the feeding behavior of the chaetognaths
1183 *Sagitta setosa* J. Müller and *S. elegans* Verril with special reference to fish eggs
1184 and larvae as food organisms. *Meeresforsch* **25:** 163-171.
1185 Lankin, K.F., Peck, M.A., Buckley, L.J., and Bengtson, D.A. (2008) The effects of
1186 temperature, body size and growth rate on energy losses due to metabolism in
1187 early life stages of haddock (*Melanogrammus aeglefinus*). *Mar. Biol*. **155:** 461-
1188 472.
1189 Lapolla, A., and Buckley, L.J. (2005) Hatch date distributions of young-of-year haddock

Melanogrammus aeglefinus in the Gulf of Maine/Georges Bank region: implications for recruitment. *Mar. Ecol. Prog. Ser.* **290:** 239-249.

Leggett, W.C., and Deblois, E. (1994) Recruitment in marine fishes: is it regulated by starvation and predation in the egg and larval stages? *Netherlands J. Sea Res.* **32:**119-134.

Lewis, C.V.W., Davis, C.S., and Gawarkiewcz, G. (1994) Wind-forced biological physical dynamics on an isolated off-shore bank. *Deep-Sea Res. II* **41:** 51-73.

Lewis, C.V.W., Chen, C., and Davis, C.S. (2001) Variability in wind forcing and its effect on circulation and plankton transport over Georges Bank. *Deep-Sea Res. II* **48:** 137-158.

Lough, R.G. (1984) Larval fish trophodynamic studies on Georges Bank: sampling strategy and initial results. In: *The propagation of cod Gadus morhua*. E. Dahl, D.S. Danielssen, E. Moskness, and P. Solemdal (eds) Flødevigen rapportser I, pp. 395-434.

Lough, R.G., and Potter, D.C. (1993) Vertical distribution patterns and diel migrations of larval and juvenile haddock *Melanogrammus aeglefinus* and Atlantic cod *Gadus morhua* on Georges Bank. *Fish. Bull.* **91:** 281-303.

Lough, R.G., Buckley, L.J., Werner, F.E., Quinlan, J.A., and Pehrson Edwards, K. (2005) A general biophysical model of larval cod (*Gadus morhua*) growth applied to populations on Georges Bank. *Fish. Oceanogr.* **14:** 241-262.

Lough, R.G., Hannah, C.G., Berrien, P., Brickman, D., Loder, J.W., and Quinlan, J.A.

(2006) Spawning pattern variability and its effect on retention, larval growth and recruitment in Georges Bank cod and haddock. *Mar. Ecol. Prog. Ser.* **310:** 193-212.

Lough, R.G., Valentine, P.C., Potter, D.C., Auditore, P.J., Bolz, G.R., Neilson, J.D., and Perry, R.I. (1989) Ecology and distribution of juvenile cod and haddock in relation to sediment type and bottom currents on eastern Georges Bank. *Mar. Ecol. Prog. Ser.* **56:** 1-12.

MacKenzie, B.R., and Kiørboe, T. (1995) Encounter rates and swimming behavior of pause-travel and cruise larval fish predators in calm and turbulent laboratory environments. *Limnol. Oceanogr*. **40:** 1278-1289.

MacKenzie, B.R., and Leggett, W.C. (1993) Wind-based models for estimating the dissipation rates of turbulent energy in aquatic environments: empirical comparisons. *Mar. Ecol. Prog. Ser.* **94:** 207-216.

Madin, L.P., Bollens, S.M., Horgan, E., Butler, M., Runge, J., Sullivan, B.K., Klein MacPhee, G., Durbin, E., Durbin, A.G., Van Keuren, D., Plourde, S., Bucklin, A., and Clarke, M.E. (1996) Voracious planktonic hydroids: unexpected predatory impact on a coastal marine ecosystem. *Deep-Sea Res. II* **43:** 1823-1829.

Mountain, D.G., and Kane, J. (2010) Major changes in the Georges Bank ecosystem, 1980s to the 1990s. *Mar. Ecol. Prog. Ser.* **398:** 81-91.

Mountain, D.G., Berrien, P., and Sibunka, J. (2003) Distribution, abundance and mortality of cod and haddock eggs and larvae on Georges Bank in 1995 and 1996. *Mar. Ecol. Prog. Ser.* **263:** 247-260.

Mountain, D., Green, J., Sibunka, J., and Johnson, D. (2008) Growth and mortality of

1234 Atlantic cod *Gadus morhua* and haddock *Melanogrammus aeglefinus* eggs and
1235 larvae on Georges Bank, 1995 to 1999. *Mar. Ecol. Prog. Ser.* **353:** 225-242.
1236 Page, F.H., and Frank, K.T. (1989) Spawning time and egg stage duration in Northwest
1237 Atlantic haddock (*Melanogrammus aeglefinus*) stocks with emphasis on Georges
1238 and Browns Bank. *Deep-Sea Res. II* **46(Suppl. 1):** 68-81.
1239 Page, F.H., Sinclair, M., Naimie, C.E., Loder, J.W., Losier, R.J., Berrien, P.L., and
1240 Lough, R.G. (1999) Cod and haddock spawning on Georges Bank in relation to
1241 water residence times. *Fish. Oceanogr.* **8:** 212-226.
1242 Papaioannou, G., Papanikolaou, N., and Retalis, D. 1993. Relationships of
1243 photosynthetically active radiation and shortwave irradiance. *Theor. Appl.*
1244 *Climatol.* **48:** 23-27.
1245 Peck, M.A., Buckley, L.J., and Bengtson, D.A. (2006) Effects of temperature and body
1246 size on the swimming speed of larval and juvenile Atlantic cod (*Gadus morhua*):
1247 implications for individual-based modeling. *Env. Biol. Fish.* **75:** 419-429.
1248 Peterson, I., and Wroblewski, J.S. (1984) Mortality rate of fishes in the pelagic
1249 ecosystem. *Deep-Sea Res. II* **41:** 1117-1120.
1250 Petrik, C.M., Kristiansen, T., Lough, R.G., and Davis, C.S. (2009) Prey selection of
1251 larval haddock and cod on copepods with species-specific behavior: a model-
1252 based analysis. *Mar. Ecol. Prog. Ser.* **396:** 123-143.
1253 Purcell, J. (1981) Feeding ecology of *Rhyzophysa eysenhardti*, a siphonophore predator
1254 of fish larvae. *Limnol. Oceanogr.* **26:** 424-432.
1255 Purcell, J. (1985) Predation on fish eggs and larvae by pelagic cnidarians and
1256 ctenophores. *Bull. Mar. Sci.* **37:** 739-755.

1257 Rideout, R.M., Trippel, E.A., and Litvak, M.K. (2005) Effects of egg size, food supply
1258 and spawning time on early life history success of haddock *Melanogrammus*
1259 *aeglefinus*. *Mar. Ecol. Prog. Ser.* **285:** 169-180.
1260 Scheffer, M., Baveco, J.M., DeAngelis, D.L., Rose, K.A., and van Nes, E.H. (1995)
1261 Super-individuals a simple solution for modeling large populations on an
1262 individual basis. *Ecol. Model.* **80:** 161-170.
1263 Sheader, M., and Evans, F. (1975) Feeding and gut structure of *Parathemisto*
1264 *gaudichaudi* (Guerin) (Amphipoda, Hyperiidea). *J. Mar. Biol. Assoc. UK* **55:** 641-
1265 656.
1266 Sheldon, R.W., Prakash, A., and Sutcliffe, Jr., W.H. (1972) The size distribution of
1267 particles in the ocean. *Limnol. Oceanogr.* **17:** 327-340.
1268 Sibunka, J.D., Johnson, D.L., and Berrien, P.L. (2006) Distribution and abundance of fish
1269 eggs collected during the GLOBEC broad-scale Georges Bank surveys, 1995-
1270 1999. *NOAA Tech. Memo. NMFS-NE* **199:** 72pp.
1271 Sullivan, B.K., and Meise, C.J. (1996) Invertebrate predators of zooplankton on Georges
1272 Bank, 1977-1987. *Deep-Sea Res. II* **43:** 1503-1519.
1273 Trippel, E.A., and Chambers, R.C. (1997) Introduction. In: *Early life history and*
1274 *recruitment in fish populations.* R.C. Chambers and E.A. Trippel (eds) London:
1275 Chapman and Hall, pp. xxi-xxxii.
1276 Vollset, K.W., Folkvord, A., and Browman, H.I. (2011) Foraging behaviour of larval cod
1277 (*Gadus morhua*) at low light intensities. *Mar. Biol.* **158:** 1125-1133.
1278 Werner, F.E., Page, F.H., Lynch, D.R., Loder, J.W., Lough, R.G., Perry, R.I., Greenberg,

D.A., and Sinclair, M. (1993) Influences of mean advection and simple behavior on the distribution of cod and haddock early life stages on Georges Bank. *Fish. Oceanogr.* **2:** 43-64.

Werner, F.E., Perry, R.I., Lough, R.G., and Naimie, C.E. (1996) Trophodynamic and advective influences on Georges Bank larval cod and haddock. *Deep-Sea Res. II* **43:** 1793-1822.

Wiebe, P., Beardsley, R., Mountain, D., and Bucklin, A. (2002) U.S. GLOBEC Northwest Atlantic/Georges Bank Program. *Oceanogr.* **15:** 13-29.

Wilcox, J.R., and Jeffries, H.P. (1974) Feeding habits of the sand shrimp *Crangon septemspinosa*. *Bio. Bull.* **146:** 424-434.

Wright, P.J., and Gibb, F.M. (2005) Selection for birth date in North Sea haddock and its relation to maternal age. *J. Anim. Ecol.* **74:** 303-312.

Yamashita, Y., Aoyama, T., and Kitagawa, D. (1985) Laboratory studies of predation by the hyperiid amphipod *Parathemisto japonica* on larvae of the Japanese sand-eel *Ammodytes personatus*. *Bull. Jap. Soc. Sci. Fish.* **50:** 1089-1093.

Yen, J. (1987) Predation by a carnivorous marine copepod, *Euchaeta norvegica* Boeck, on eggs and larvae of the North Atlantic cod *Gadus morhua* L. *J. Exp. Mar. Biol. Ecol.* **112:** 283-296.

TABLES

Table 1. Statistics on the number of individuals (n) per super-individual (super) at time of hatch.

	1995			1998		
	Feb	Mar	Apr	Feb	Mar	Apr
Min.(n)	6.50×10^5	7.10×10^5	6.96×10^5	6.43×10^5	7.14×10^5	1.37×10^6
Max.(n)	2.37×10^9	2.42×10^{10}	6.24×10^9	1.99×10^{10}	2.31×10^{10}	2.11×10^{10}
Mean(n)	1.62×10^8	1.06×10^9	6.74×10^8	1.09×10^9	2.22×10^9	2.52×10^9
Std. Dev.(n)	3.22×10^8	2.22×10^9	1.02×10^9	2.04×10^9	3.87×10^9	3.35×10^9
Total(n)	4.81×10^{11}	4.47×10^{12}	1.80×10^{12}	3.90×10^{12}	3.47×10^{12}	1.42×10^{13}
Annual total(n)		6.75×10^{12}			2.85×10^{13}	
Total(super)	2.97×10^3	4.22×10^3	2.67×10^3	3.59×10^3	4.69×10^3	5.63×10^3
Annual total(super)		9.86×10^3			1.39×10^4	

Table 2. The different simulations, their notation, the variable or process changed, and the hypothesis tested with each.

Case name	Notation	Changed	Hypothesis tested
Reference	R	--	Interannual recruitment variability; hatch date of survivors
Cross initialization	O	Physical environment	Hatch location vs. physical environment during transport
Low prey	L	1998 prey densities	Food-limitation
Swimming behavior	DVM	Vertical swimming	Effect of vertical distribution
Temperature-dependent predation	TP6	Total predation rate T_{base}=6.5°C	Seasonal increases in predation rate
	TP5	T_{base}=5.5°C	
Spatially-dependent predation	CP	Total predation rate C+50%, F-50%	Spatially distinct predator communities
	FP	C-50%, F+50%	
Interannually varying predation	95P+	Total predation rate 95+10%, 98-10%	Interannually different predation rates
	95P-	95-10%, 98+10%	

Table 3. Weighted mean time (d) to 12 mm and weighted mean specific growth rate (d^{-1}) of individuals from hatch until survival to 12 mm in the reference case. Mean time calculations include individuals that reached 12 mm after the 55 d larval period, but the mean growth rates do not.

	Feb		Mar		Apr	
1995	51	0.041	46	0.051	46	0.042
1998	48	0.054	47	0.049	38	0.062

Table 4. Fate, contribution of each cohort, and annual survival of individuals (as fraction of total individuals hatched) at 55 dph or 12 mm in the reference case with systematic addition of mortality sources.

		1995			1998		
		F	M	A	F	M	A
Advection only	Advection	0.03	0.13	0.11	0.06	0.24	0.27
	Survival	0.97	0.87	0.89	0.94	0.76	0.73
	Cohort contribution	0.08	0.65	0.27	0.17	0.36	0.47
	Survival per hatch		0.88			0.77	
Advection and starvation only	Advection	0.03	0.13	0.11	0.06	0.24	0.27
	Starvation	0.89	0.71	0.44	0.82	0.57	0.32
	Survival	0.08	0.16	0.45	0.12	0.19	0.41
	Cohort contribution	0.03	0.46	0.52	0.06	0.24	0.71
	Survival per hatch		0.23			0.29	
All sources	Advection	0.01	0.07	0.09	0.04	0.15	0.16
	Starvation	0.49	0.24	0.20	0.39	0.21	0.12
	Predation	0.49	0.69	0.69	0.57	0.63	0.68
	Survival	0.003	0.003	0.022	0.005	0.006	0.036
	Cohort contribution	0.02	0.27	0.71	0.03	0.11	0.86
	Survival per hatch		0.01			0.02	

Table 5. Total number of surviving larvae ($\times 10^{10}$) by cohort in the reference case.

	Feb	Mar	Apr	Total
1995	0.14	1.51	4.01	5.66
1998	1.91	6.23	50.47	58.61

Table 6. Weighted mean temperature (°C) experienced by individuals from hatch until survival to 12 mm for each cohort in the reference case.

	Feb	Mar	Apr
1995	6.5	6.4	7.0
1998	6.4	6.4	7.4

Table 7. Weighted mean *Pseudocalanus* spp. concentration (no. m^{-3}) of the grouped developmental stages experienced by individuals from hatch until survival to 12 mm for each cohort and year in the reference case.

	1995 reference			1998 reference			1998 low prey		
	Feb	Mar	Apr	Feb	Mar	Apr	Feb	Mar	Apr
Nauplii	472	983	2085	692	1815	4552	357	1035	2333
Copepodites	231	315	416	490	594	1471	300	354	761
Adults	22	62	93	41	108	222	22	69	111
Total	726	1360	2594	1223	2517	6245	679	1458	3204

Table 8. Fate of all individuals, as fraction of total individuals hatched, at 55 dph or 12 mm in the reference and cross-initialization cases.

		1995 environment			1998 environment		
		Feb	Mar	Apr	Feb	Mar	Apr
1995 hatch	Advection	0.01	0.07	0.09	0.01	0.03	0.11
	Starvation	0.49	0.24	0.20	0.38	0.20	0.13
	Predation	0.49	0.69	0.69	0.61	0.76	0.73
	Survived	0.003	0.003	0.022	0.006	0.009	0.028
1998 hatch	Advection	0.08	0.24	0.12	0.04	0.15	0.16
	Starvation	0.46	0.24	0.21	0.39	0.21	0.12
	Predation	0.47	0.51	0.64	0.57	0.63	0.68
	Survived	0.001	0.003	0.032	0.005	0.006	0.036

1441 **FIGURE CAPTIONS**

1442 **Fig. 1.** Map of the Gulf of Maine (GOM) and Georges Bank with the subregions: Crest
1443 (C), Great South Channel (GSC), Mid-Atlantic Bight (MAB), Northeast Peak (NEP),
1444 Northern Flank (NF), and Southern Flank (SF). The 60, 100, and 200 m isobaths are
1445 shown and labeled.

1446

1447 **Fig. 2.** 1995 reference case distributions of individuals at hatch (a-c), of all individuals,
1448 dead or alive, at the weighted mean time to 12 mm (d-f), and of individuals that survived
1449 to 12 mm at the weighted mean time to 12 mm (g-i). The gray lines are the 60, 100, and
1450 200 m isobaths. Hatch locations were determined from observations of egg abundance
1451 (Sibunka *et al.*, 2006) projected forward using estimated egg mortality rates and spatially
1452 integrated kriging as described in Mountain *et al.* (2003, 2008). Contours are presented
1453 for the log of the fraction of individuals.

1454

1455 **Fig. 3.** 1998 reference case distributions of individuals at hatch (a-c), of all individuals,
1456 dead or alive, at the weighted mean time to 12 mm (d-f), and of individuals that survived
1457 to 12 mm at the weighted mean time to 12 mm (g-i). The gray lines are the 60, 100, and
1458 200 m isobaths. Hatch locations were determined from observations of egg abundance
1459 (Sibunka *et al.*, 2006) projected forward using estimated egg mortality rates and spatially
1460 integrated kriging as described in Mountain *et al.* (2003, 2008). Contours are presented
1461 for the log of the fraction of individuals.

1462

1463 **Fig. 4.** Percent contributed by each cohort to the total number of individuals (top) hatched
1464 and (bottom) survived to 55 dph or 12 mm in the reference case. F: February (black), M:
1465 March (gray), A: April (white).
1466
1467 **Fig. 5.** Weighted mean depth of larvae from 1995 (a-d) and 1998 (e-h) hatch until 55 dph
1468 or 12 mm in 10 m depth bins. Passive: reference, DVM: diel vertical migration, All: all
1469 larvae, 12 mm: only those that survived to 12 mm.
1470
1471 **Fig. 6.** Fate of all individuals, as percent of total individuals hatched, at 55 dph or 12 mm
1472 in the reference and cross-initialization cases. A: advection, P: predation, St: starvation,
1473 Su: survived.
1474
1475 **Fig. 7.** Fate of all individuals, as percent of total individuals hatched west or east of
1476 67.5°W, at 55 dph or 12 mm in the reference case. A: advection, P: predation, St:
1477 starvation, Su: survived.
1478
1479 **Fig. 8.** Percent contributed by each cohort to the total number of individuals (top) hatched
1480 west or east of 67.5°W and (bottom) survived to 55 dph or 12 mm in the reference case.
1481 F: February, M: March, A: April, W: west, E: east.
1482
1483 **Fig. 9.** (a) Survival per hatch (fraction of individuals that survived to 55 dph or 12 mm
1484 out of all those hatched) in 1995 and 1998 for all ten cases. The dashed lines are the 1995
1485 and 1998 reference case values. (b) 1998:1995 ratio of the number of survivors per

hatched larva. The dashed line at 1.17 represents the calculated 1998:1995 ratio of the number of recruits per hatch from Mountain and Kane (2010). R: reference, O: opposite environment, DVM: diel vertical migration behavior, CP: spatially-dependent high crest predation, FP: spatially-dependent high flank predation, 95P+: higher 1995 predation, 95P-: lower 1995 predation, TP6: temperature-dependent predation T_{base}=6.5°C, TP5: temperature-dependent predation T_{base}=5.5°C, L: low prey.

Fig. 10. The fraction of individuals hatched that were lost to (a) advection, (b) predation, and (c) starvation in 1995 and 1998. Note differences in y-axis scales. The dashed lines are the 1995 and 1998 reference case values. R: reference, O: opposite environment, DVM: diel vertical migration behavior, CP: spatially-dependent high crest predation, FP: spatially-dependent high flank predation, 95P+: higher 1995 predation, 95P-: lower 1995 predation, TP6: temperature-dependent predation T_{base}=6.5°C, TP5: temperature-dependent predation T_{base}=5.5°C, L: low prey.

Fig. 11. Fraction of surviving individuals from each cohort (cohort contribution) is presented as the difference from the reference case for 1995 (a-c) and 1998 (d-f). O: opposite environment, D: diel vertical migration behavior, C: spatially-dependent high crest predation, F: spatially-dependent high flank predation, P+: higher 1995 predation, P-: lower 1995 predation, TP6: temperature-dependent predation T_{base}=6.5°C, TP5: temperature-dependent predation T_{base}=5.5°C, L: low prey.

Fig. 12. Weighted mean specific growth rate (d^{-1}) of surviving 12 mm individuals from all cohorts in 1995 and 1998. The dashed lines are the 1995 and 1998 reference case values. R: reference, O: opposite environment, DVM: diel vertical migration behavior, CP: spatially-dependent high crest predation, FP: spatially-dependent high flank predation, 95P+: higher 1995 predation, 95P-: lower 1995 predation, TP6: temperature-dependent predation T_{base}=6.5°C, TP5: temperature-dependent predation T_{base}=5.5°C, L: low prey.

Fig. 13. Mean log abundance and standard errors (m^{-3}) of the potential predators (a) mysid shrimps, (b) siphonophores, and (c) hyperiid amphipods on Georges Bank in 1995 (solid line) and 1998 (dashed line).

Fig. 14. Comparison of Buckley and Durbin (2006) derived curves (lines) to model weighted mean specific growth rates (d^{-1}) of 12 mm survivors and the weighted mean prey concentrations they experienced for (a) 5-7 mm and (b) 7-12 mm larvae. 1995 reference (circle), 1998 reference (diamond), 1998 low prey (plus). Note the differences in x- and y-axis scales in (a) and (b).

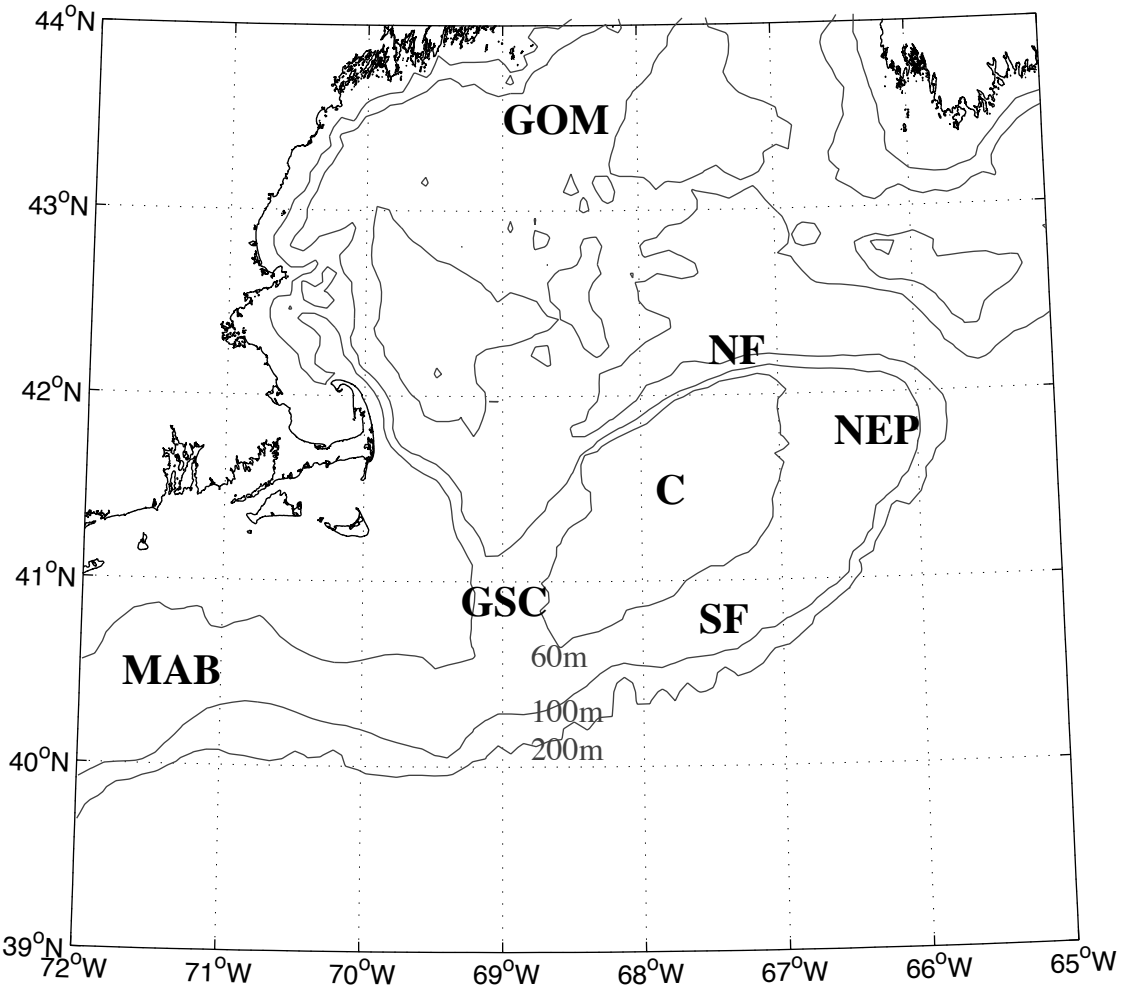

Fig. 1. Map of the Gulf of Maine (GOM) and Georges Bank with the subregions: Crest (C), Great South Channel (GSC), Mid-Atlantic Bight (MAB), Northeast Peak (NEP), Northern Flank (NF), and Southern Flank (SF). The 60, 100, and 200 m isobaths are shown and labeled.

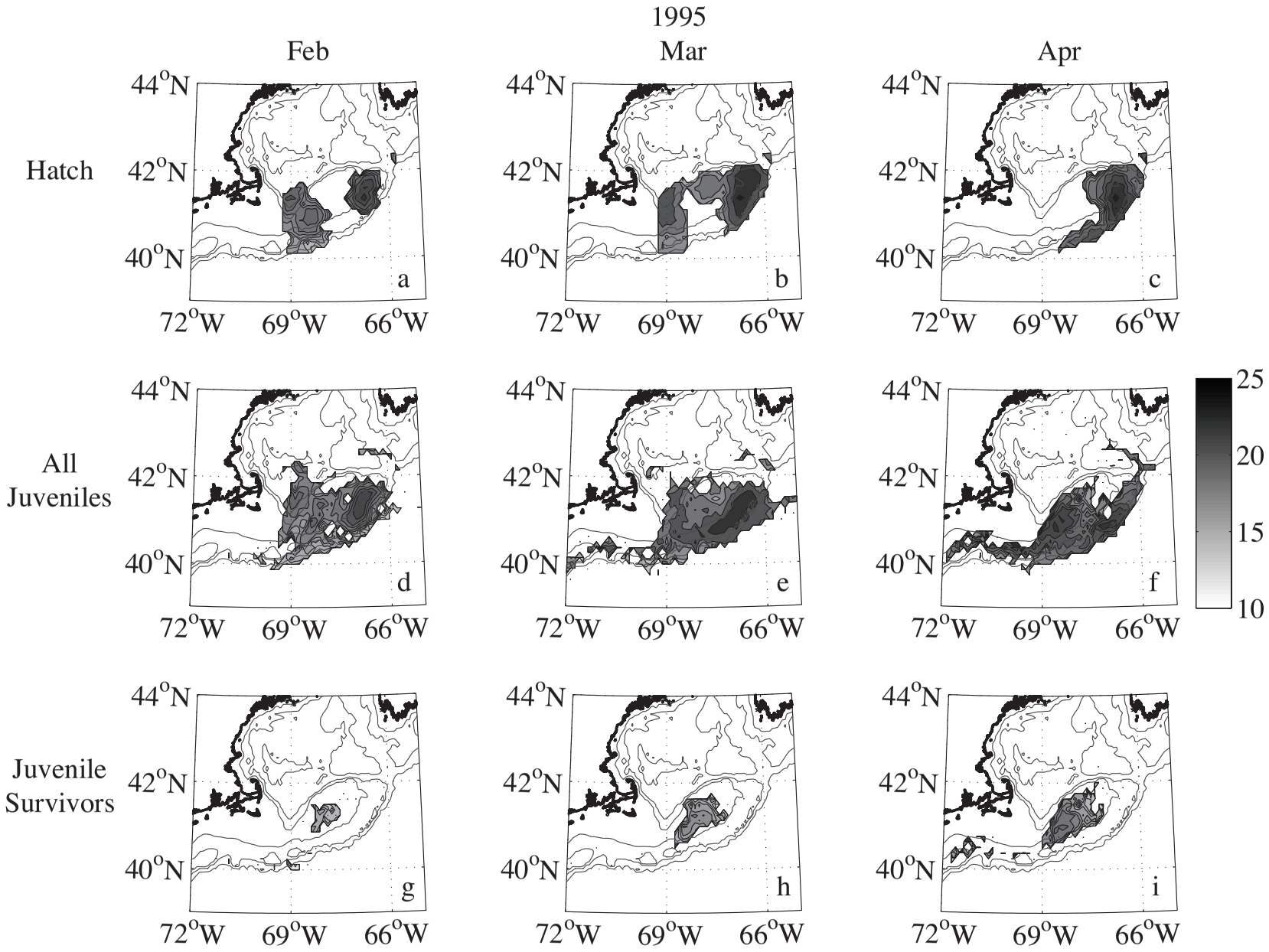
1995
Feb
Mar
Apr
Hatch
All
Juveniles
Juvenile
Survivors
44°N
42°N
40°N
72°W
69°W
66°W
a
b
c
d
e
f
g
h
i
25
20
15
10

Fig. 2. 1995 reference case distributions of individuals at hatch (a-c), of all individuals, dead or alive, at the weighted mean time to 12 mm (d-f), and of individuals that survived to 12 mm at the weighted mean time to 12 mm (g-i). The gray lines are the 60, 100, and 200 m isobaths. Hatch locations were determined from observations of egg abundance (Sibunka *et al.*, 2006) projected forward using estimated egg mortality rates and spatially integrated kriging as described in Mountain *et al.* (2003, 2008). Contours are presented for the log of the fraction of individuals.

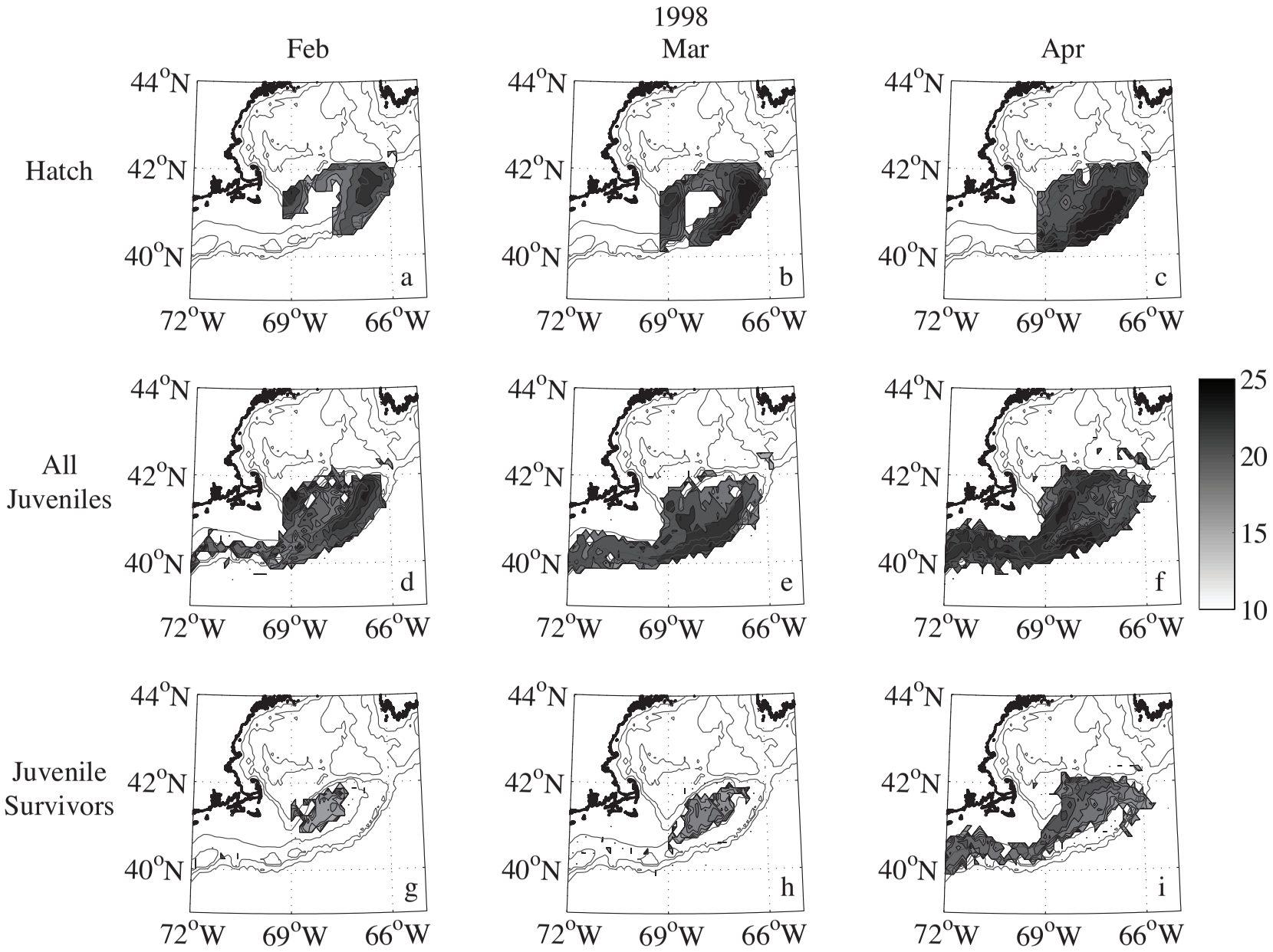
1998
Feb
Mar
Apr
Hatch
All
Juveniles
Juvenile
Survivors
44°N
42°N
40°N
72°W
69°W
66°W
a
b
c
d
e
f
g
h
i
25
20
15
10

Fig. 3. 1998 reference case distributions of individuals at hatch (a-c), of all individuals, dead or alive, at the weighted mean time to 12 mm (d-f), and of individuals that survived to 12 mm at the weighted mean time to 12 mm (g-i). The gray lines are the 60, 100, and 200 m isobaths. Hatch locations were determined from observations of egg abundance (Sibunka *et al.*, 2006) projected forward using estimated egg mortality rates and spatially integrated kriging as described in Mountain *et al.* (2003, 2008). Contours are presented for the log of the fraction of individuals.

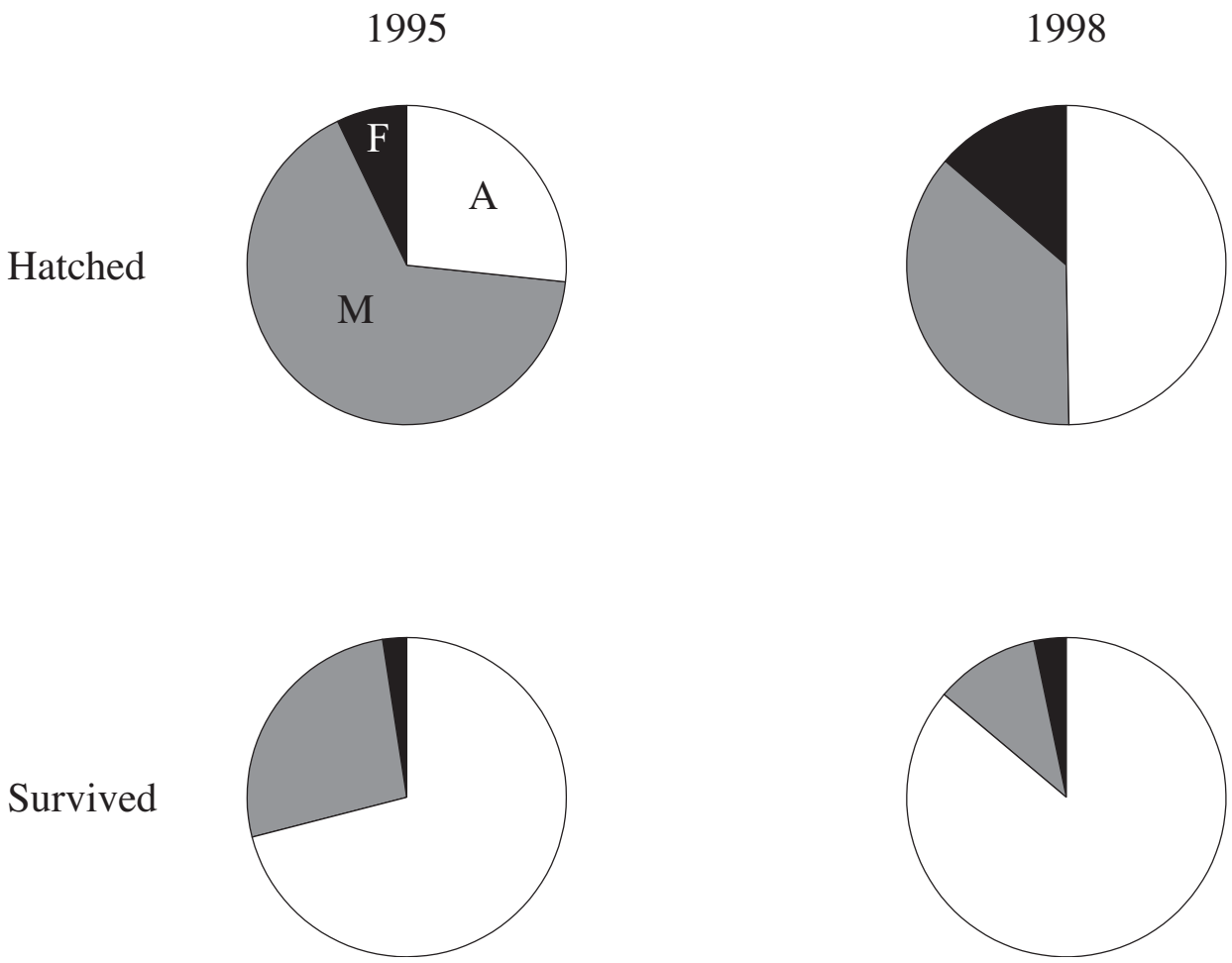

Fig. 4. Percent contributed by each cohort to the total number of individuals (top) hatched and (bottom) survived to 55 dph or 12 mm in the reference case. F: February (black), M: March (gray), A: April (white).

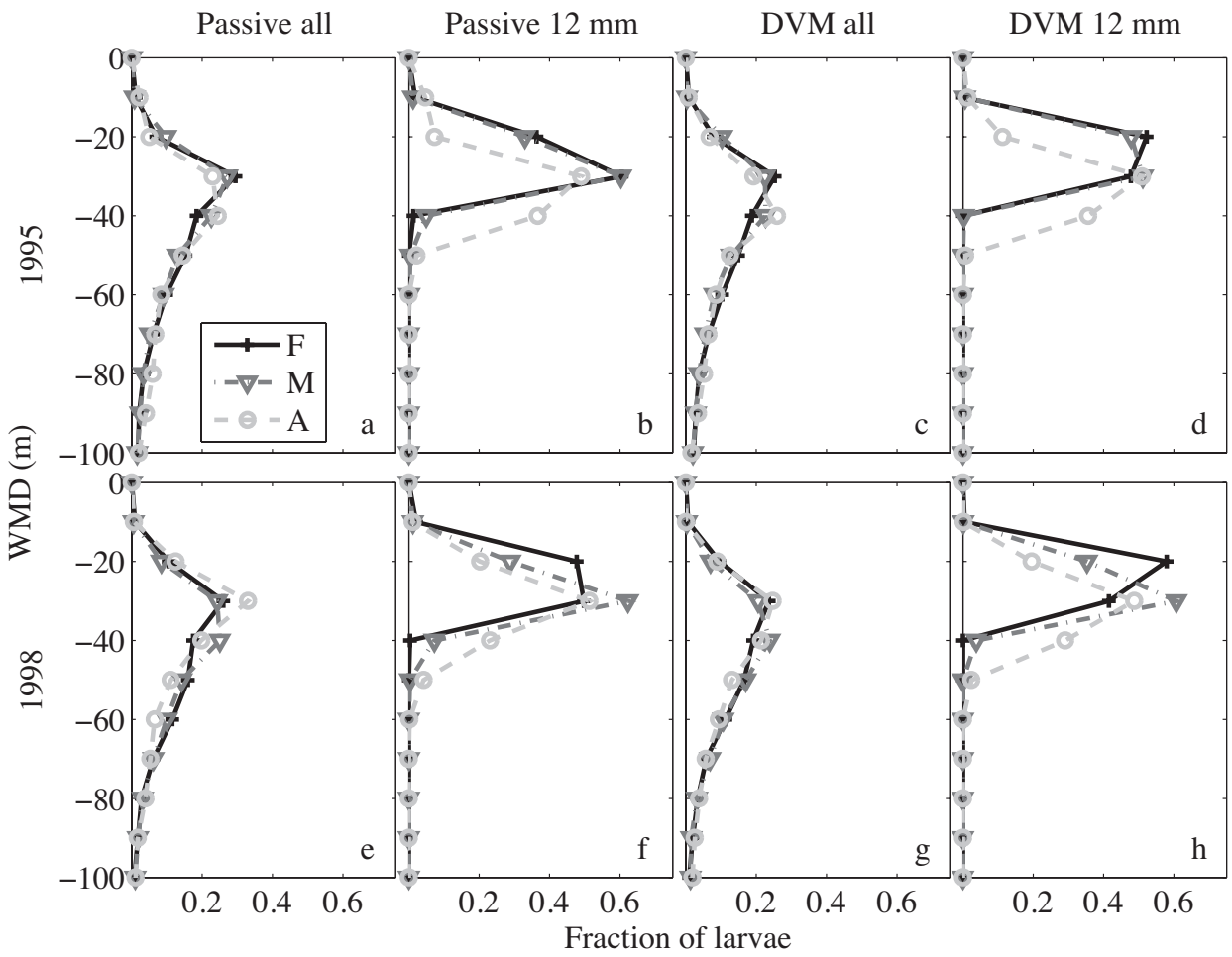

Fig. 5. Weighted mean depth of larvae from 1995 (a-d) and 1998 (e-h) hatch until 55 dph or 12 mm in 10 m depth bins. Passive: reference, DVM: diel vertical migration, All: all larvae, 12 mm: only those that survived to 12 mm.

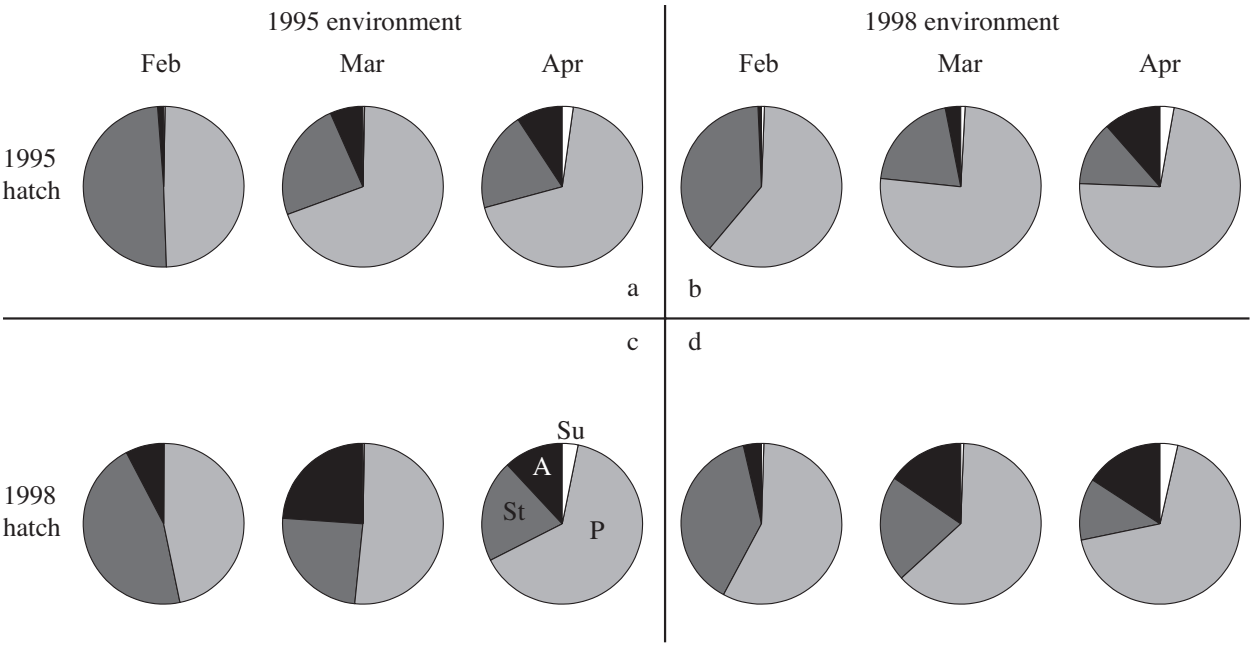

Fig. 6. Fate of all individuals, as percent of total individuals hatched, at 55 dph or 12 mm in the reference and cross-initialization cases. A: advection, P: predation, St: starvation, Su: survived.

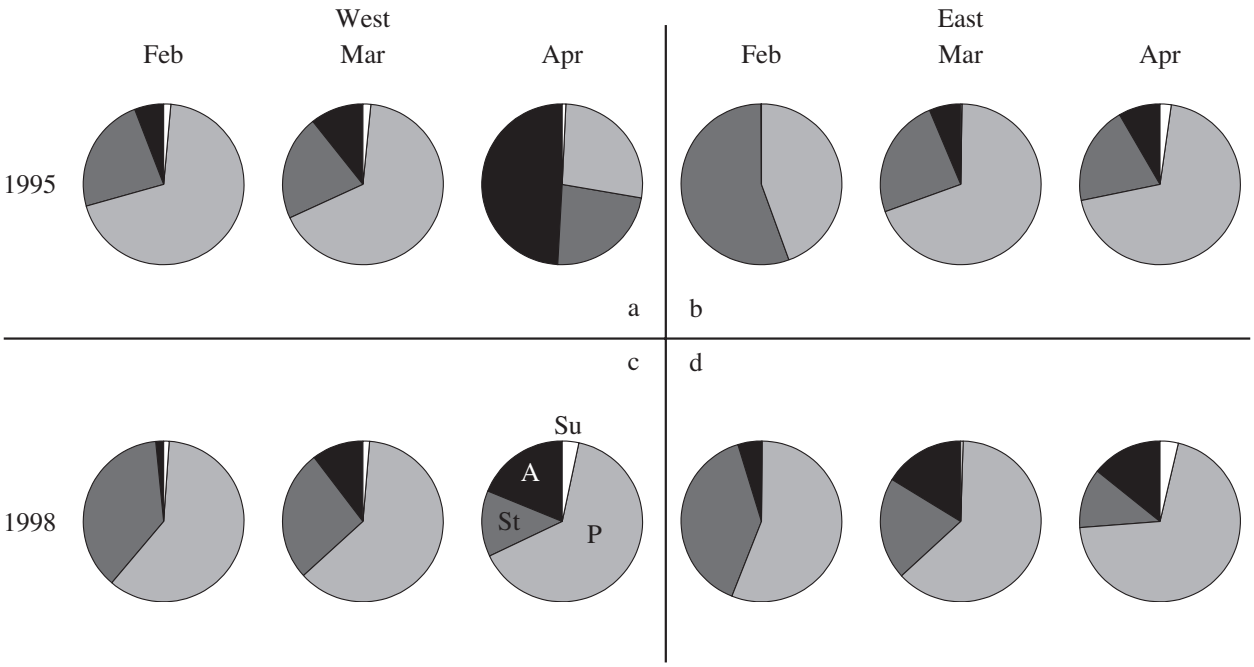

Fig. 7. Fate of all individuals, as percent of total individuals hatched west or east of 67.5°W, at 55 dph or 12 mm in the reference case. A: advection, P: predation, St: starvation, Su: survived.

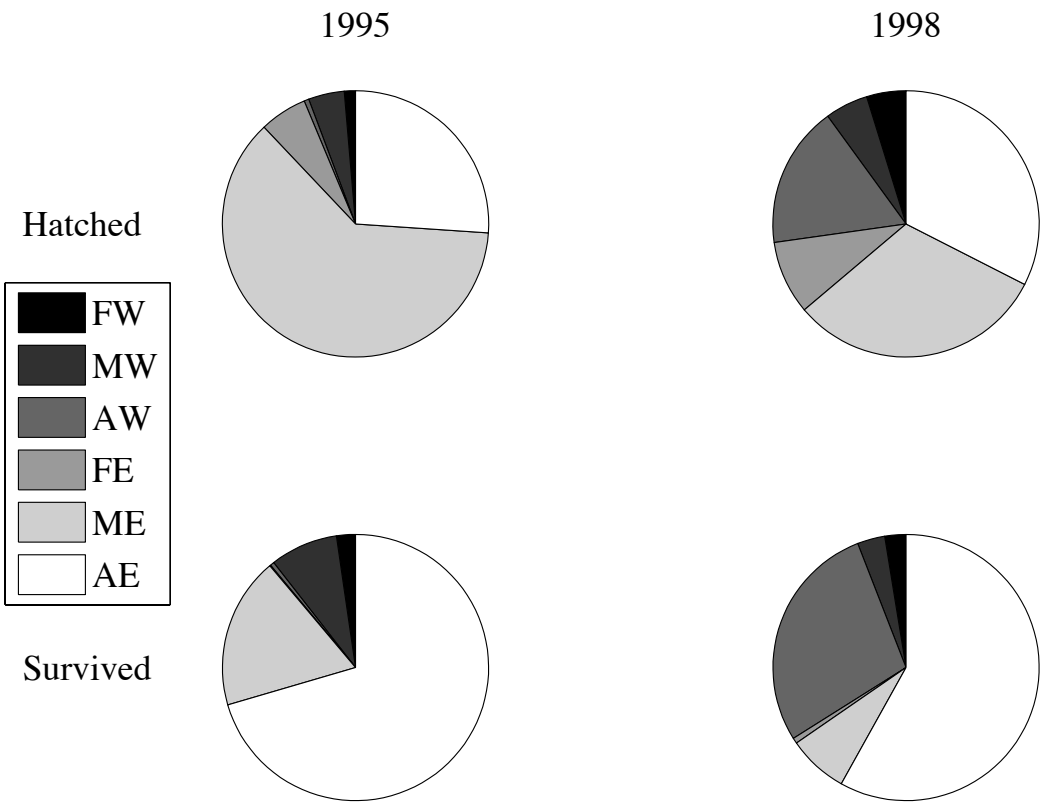

Fig. 8. Percent contributed by each cohort to the total number of individuals (top) hatched west or east of 67.5°W and (bottom) survived to 55 dph or 12 mm in the reference case. F: February, M: March, A: April, W: west, E: east.

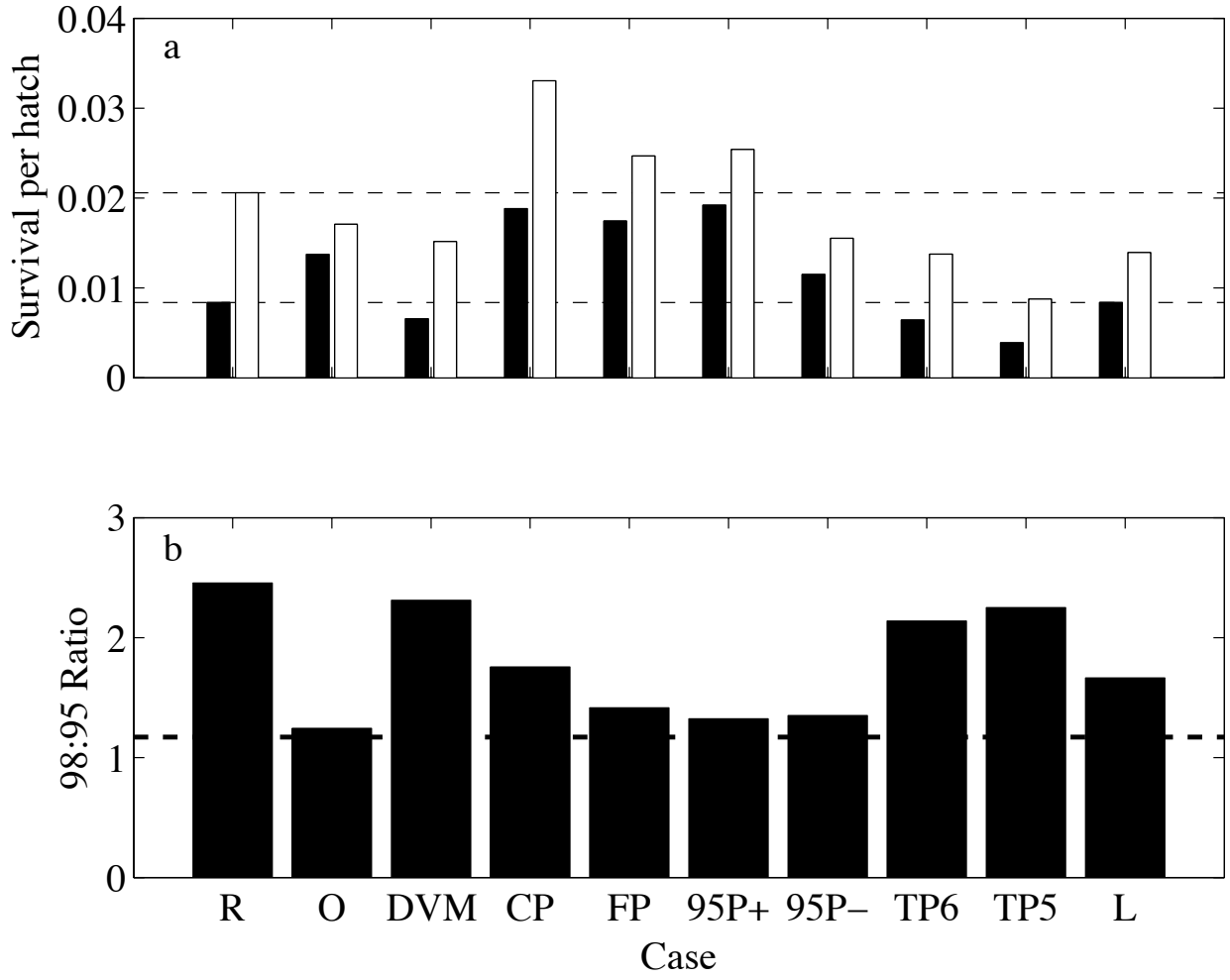

Fig. 9. (a) Survival per hatch (fraction of individuals that survived to 55 dph or 12 mm out of all those hatched) in 1995 and 1998 for all ten cases. The dashed lines are the 1995 and 1998 reference case values. (b) 1998:1995 ratio of the number of survivors per hatched larva. The dashed line at 1.17 represents the calculated 1998:1995 ratio of the number of recruits per hatch from Mountain and Kane (2010). R: reference, O: opposite environment, DVM: diel vertical migration behavior, CP: spatially-dependent high crest predation, FP: spatially-dependent high flank predation, 95P+: higher 1995 predation, 95P-: lower 1995 predation, TP6: temperature-dependent predation T_{base}=6.5°C, TP5: temperature-dependent predation T_{base}=5.5°C, L: low prey.

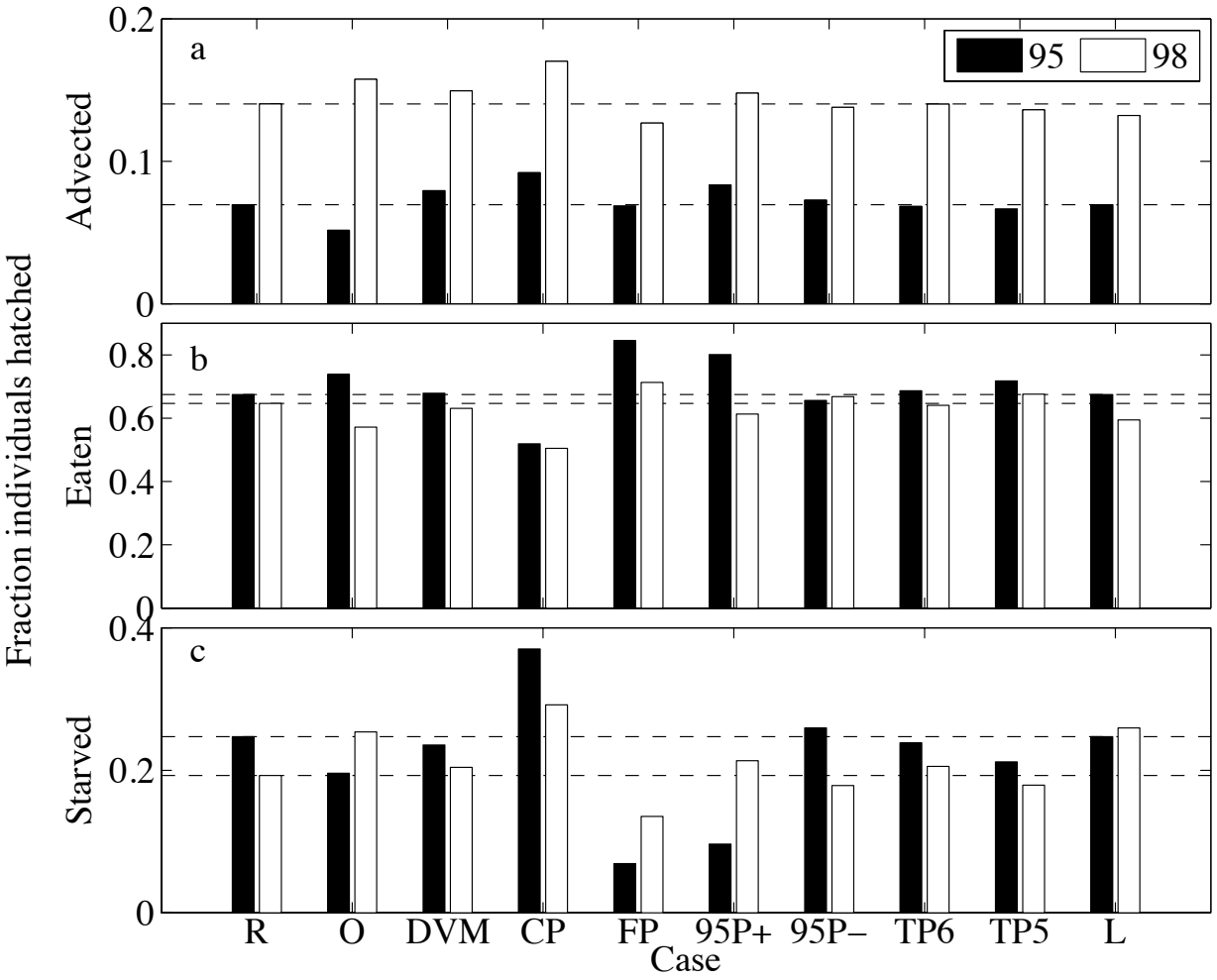

Fig. 10. The fraction of individuals hatched that were lost to (a) advection, (b) predation, and (c) starvation in 1995 and 1998. Note differences in y-axis scales. The dashed lines are the 1995 and 1998 reference case values. R: reference, O: opposite environment, DVM: diel vertical migration behavior, CP: spatially-dependent high crest predation, FP: spatially-dependent high flank predation, 95P+: higher 1995 predation, 95P-: lower 1995 predation, TP6: temperature-dependent predation T_{base}=6.5°C, TP5: temperature-dependent predation T_{base}=5.5°C, L: low prey.

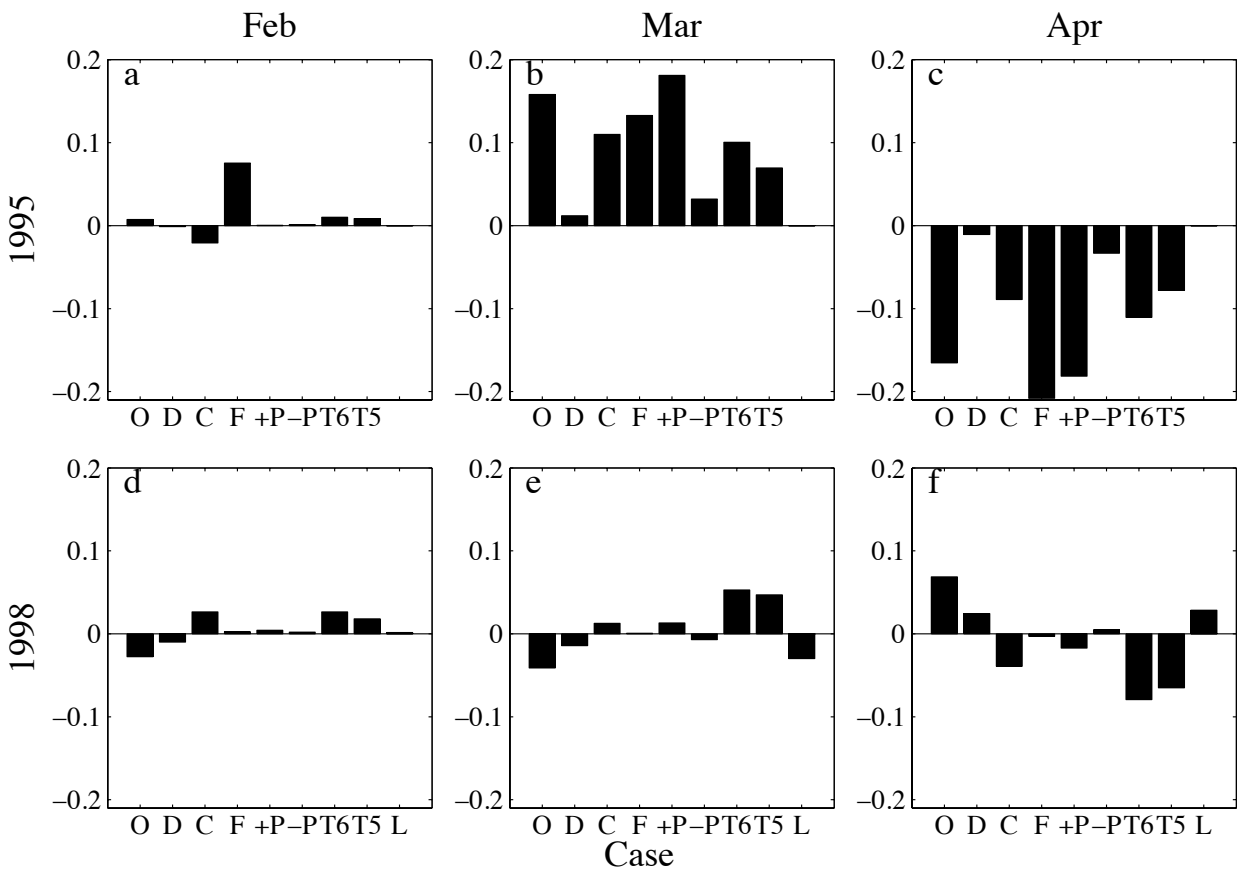

Fig. 11. Fraction of surviving individuals from each cohort (cohort contribution) is presented as the difference from the reference case for 1995 (a-c) and 1998 (d-f). O: opposite environment, D: diel vertical migration behavior, C: spatially-dependent high crest predation, F: spatially-dependent high flank predation, P+: higher 1995 predation, P-: lower 1995 predation, TP6: temperature-dependent predation T_{base}=6.5°C, TP5: temperature-dependent predation T_{base}=5.5°C, L: low prey.

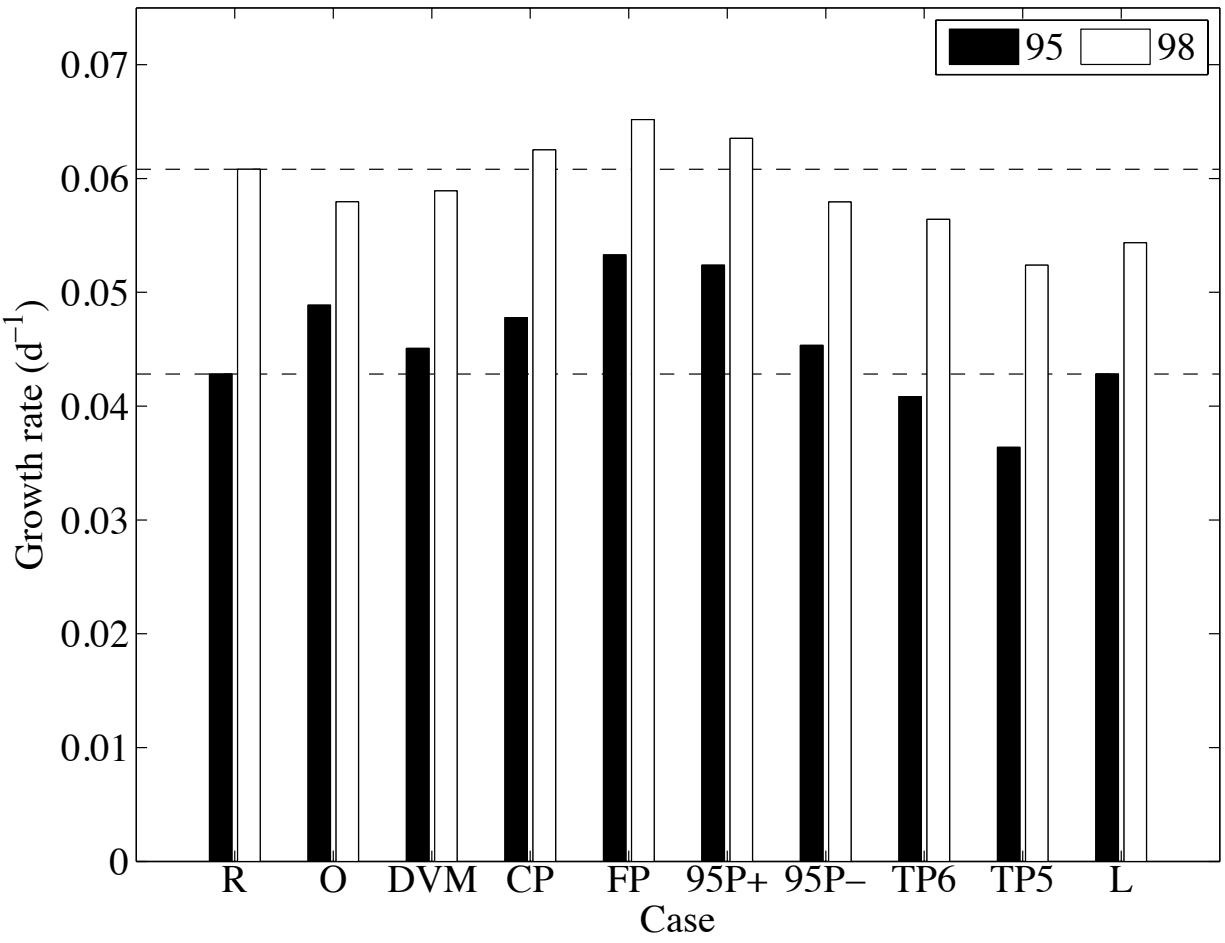

Fig. 12. Weighted mean specific growth rate (d^{-1}) of surviving 12 mm individuals from all cohorts in 1995 and 1998. The dashed lines are the 1995 and 1998 reference case values. R: reference, O: opposite environment, DVM: diel vertical migration behavior, CP: spatially-dependent high crest predation, FP: spatially-dependent high flank predation, 95P+: higher 1995 predation, 95P-: lower 1995 predation, TP6: temperature-dependent predation T_{base}=6.5°C, TP5: temperature-dependent predation T_{base}=5.5°C, L: low prey.

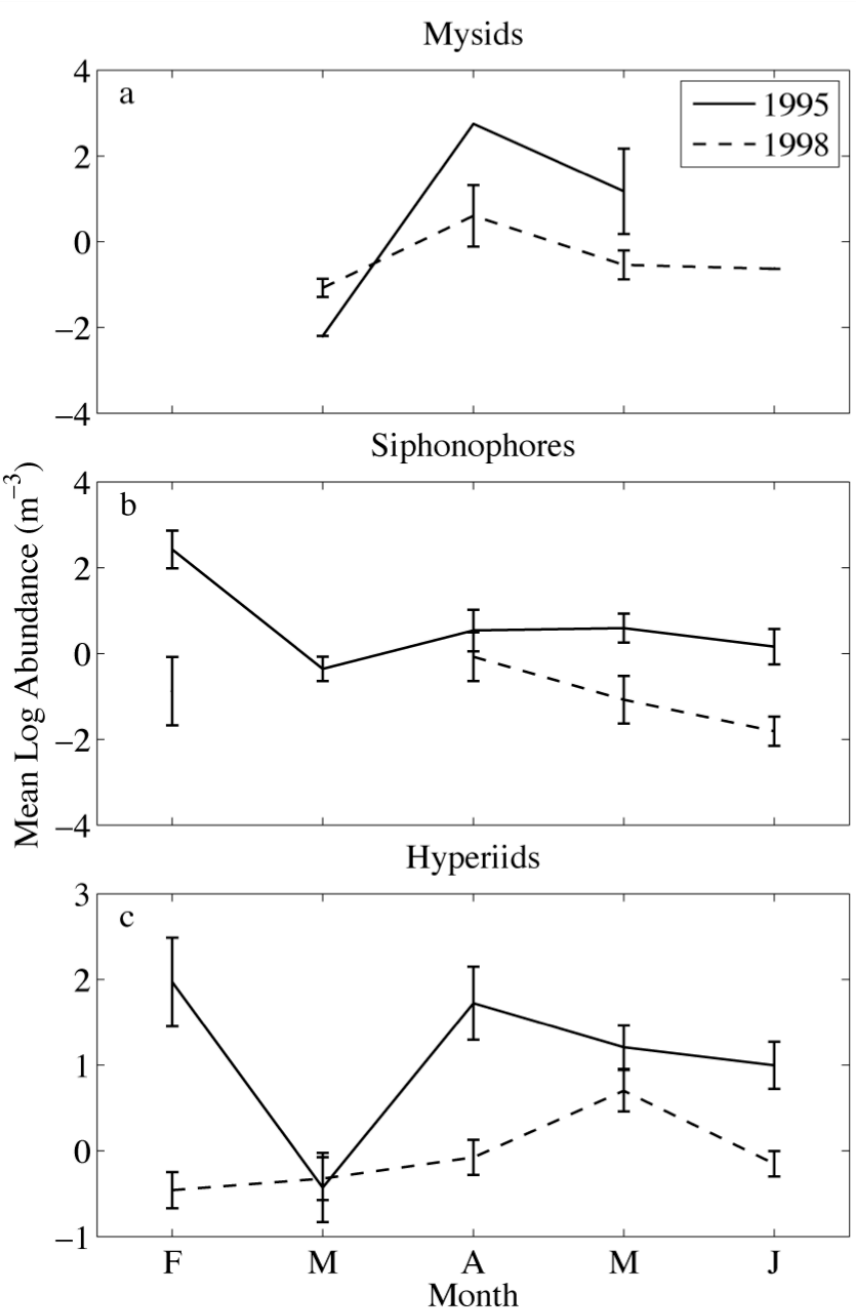

Fig. 13. Mean log abundance and standard errors (m^{-3}) of the potential predators (a) mysid shrimps, (b) siphonophores, and (c) hyperiid amphipods on Georges Bank in 1995 (solid line) and 1998 (dashed line).

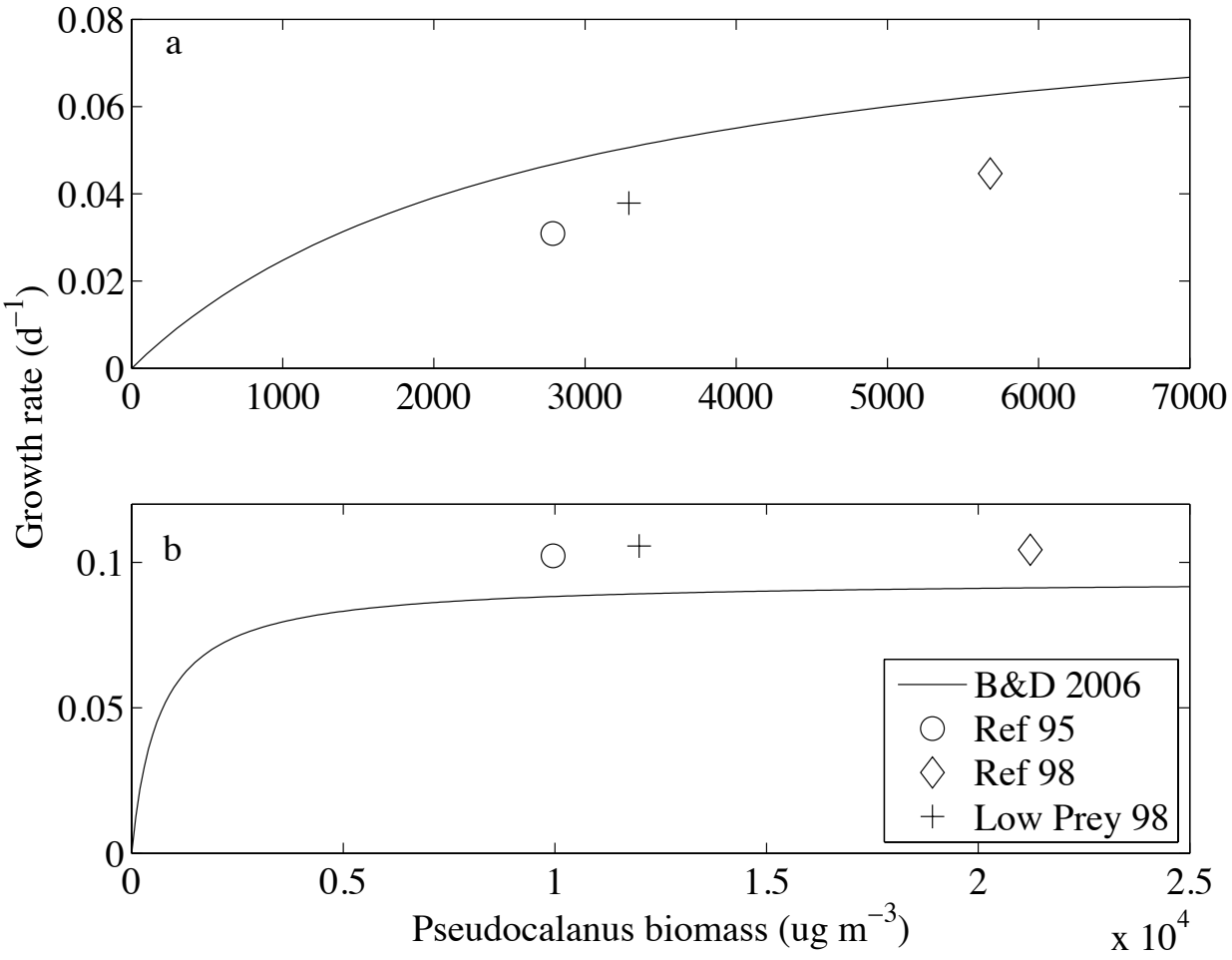

Fig. 14. Comparison of Buckley and Durbin (2006) derived curves (lines) to model weighted mean specific growth rates (d^{-1}) of 12 mm survivors and the weighted mean prey concentrations they experienced for (a) 5-7 mm and (b) 7-12 mm larvae. 1995 reference (circle), 1998 reference (diamond), 1998 low prey (plus). Note the differences in x- and y-axis scales in (a) and (b).

APPENDIX: Model equations

All parameters and variables are defined in Table A1.

Prey density

The *Pseudocalanus* spp. density was modeled with a 4-stage (eggs-nauplii-copepodite-adult) concentration-based population model (Hu *et al.*, 2008; Ji *et al.*, 2009), excluding the eggs as a prey source. Individual-based model copepod density, $prey_{dens,i}$ (mm^{-3}), was calculated from the *Pseudocalanus* spp. population model density, $ENCA_i$ (m^{-3}), for each developmental stage *i* (N, C, A) according to the following.

For all 1995 simulations,

$$prey_{dens,i} = 10^{-9} \cdot \mathrm{ENCA}_i. \quad [1]$$

For the 1998 low prey simulation,

$$prey_{dens,i} = 2.5 \cdot 10^{-9} \cdot \mathrm{ENCA}_i. \quad [2]$$

For all other 1998 simulations,

$$prey_{dens,i} = 5.0 \cdot 10^{-9} \cdot \mathrm{ENCA}_i. \quad [3]$$

Copepod characteristics

The length, width, and biomass of a grouped developmental stage was set as the mean of all stages within that group using the stage-specific lengths, l_{cope} (mm), widths, *width* (mm), and biomasses, *biom* (μg), in Davis (1984, 1987) (Table A2). The copepod image area, A_{cope} (mm), was

$$A_{cope} = 0.75 \cdot l_{cope} \cdot width, \quad [4]$$

and the *Pseudocalanus* spp. specific swimming speed, *u* ($mm\ s^{-1}$), was

$$u = 0.859 \cdot l_{cope}. \quad [5]$$

Light

Visible surface light, PAR (μmol m^{-2} s^{-1}), was estimated from the physical model output of shortwave radiation, *swrad* (μmol m^{-2} s^{-1}),

$$\mathrm{PAR} = 0.45 \cdot swrad \quad [6]$$

A ratio of PAR to shortwave radiation of 0.45 is representative of field measurements (c.f. Papaioannou *et al.*, 1993). In situ light, *E(z)* (μmol m^{-2} s^{-1}), decayed with depth;

$$E(z) = \mathrm{PAR} \cdot e^{-z \cdot att}, \quad [7]$$

with an attenuation coefficient, *att* (m^{-1}), characteristic of the Gulf of Maine/Georges Bank region.

Larval visual range

Larval eye sensitivity, E_l, was a function of its length,

$$E_l = \frac{l^2}{0.015}. \quad [8]$$

and was used in the calculation of visual range, R_{larva} (mm),

$$R_{larva}^2 = C \cdot A_{cope} \cdot E_l \cdot \exp(-c \cdot R) \cdot \frac{E(z)}{K_e + E(z)}, \quad [9]$$

also a function of prey contrast, *C*, copepod image area, the scattering of image-forming light, *c*, in situ light, and the larval light half saturation value, K_e (μmol m^{-2} s^{-1}).

Turbulence

Turbulent kinetic energy, *tke* (m^2 s^{-3}), was related to the vertical diffusivity, *kh* (m^2 s^{-1}), from the physical model,

$$tke = 1.6 \cdot 10^{-5} \cdot kh, \quad [10]$$

and was used to calculate the turbulent velocity, ω (mm s^{-1}),

$$\omega = 10^{-3} \cdot \sqrt{3.615 \cdot (tke \cdot (R_{larva} \cdot 10^{-3}))^{2/3}}. \quad [11]$$

Probability of successful capture

The probability of successful capture, p_{cap}, was an empirical function of prey species (*Pseudocalanus* spp.) and stage length fit to the results of mechanistic simulations of species-specific prey escape behaviors, which included the deformation rate threshold, escape jump speed, and escape jump angle, such that

$$p_{cap} = \frac{\exp(d_1 \cdot r^3 + d_2 \cdot r^2 + d_3 \cdot r + d_4)}{1 + \exp(d_1 \cdot r^3 + d_2 \cdot r^2 + d_3 \cdot r + d_4)}, \quad [12]$$

where *d*'s are species-specific constants, and *r* is the copepod prey to larval fish length ratio.

Encounter rate

If $p_{cap} < 0.05$, then the number of prey encountered, *enc* (mm^{-3}), was zero. Otherwise, the number of prey encountered per time step, *dt*, was a function of prey density, larval pause frequency, *f* (s^{-1}), larval pause duration, τ (s), larval visual range, copepod swimming speed, and turbulent velocity,

$$enc = prey_{dens} \cdot \left(\frac{2}{3}\pi \cdot f \cdot R_{larva}^3 + \pi \cdot f \cdot \tau \cdot R_{larva}^2 \cdot \sqrt{u^2 \cdot \omega^2}\right) \cdot dt. \quad [13]$$

Ingestion

Each copepod developmental stage was encountered and captured separately. The number of each stage captured, *cap*, and the biomass of each stage ingested, $ingest_i$ (µg), for each stage were

$$cap = enc \cdot p_{cap}, \quad [14]$$

$$ingest_i = cap \cdot biom. \quad [15]$$

Total ingestion, $ingest_{tot}$ (µg), was the sum of the biomass ingested of each copepod developmental stage;

$$ingest_{tot} = \sum_i^{N,C,A} ingest_i. \quad [16]$$

A fraction of the ingested biomass was assimilated using a size-dependent assimilation efficiency, *assim*,

$$assim = 0.8 \cdot (1.0 - 0.4 \cdot \exp(-0.002 \cdot (m_{\mu g} - 50.0))) \cdot dt/3600. \quad [17]$$

The assimilated biomass moved into the stomach, but was limited by the amount of room available in the stomach from the previous time step. The new gut contents, *gut* (µg), became

$$gut_t = gut_{t-dt} + assim \cdot ingest_{tot} \quad [18]$$

if they were less than the size of the larval gut. Otherwise, they were the size of the gut, which was 6% of the larval mass.

Metabolism

The routine respiration rate, *metab* (µg), of haddock was set as

$$metab_r = 1.021 \cdot m_{mg}^{0.979} \cdot e^{0.092 \cdot T} \cdot dt/3600, \quad [19]$$

where *T* is temperature in ºC. Metabolism was increased a constant amount during light hours to account for the swimming activity of feeding fish. The light threshold was

updated to reflect the recent findings of active feeding at low light intensities. The light threshold was 5.0×10^{-3} µmol m^{-2} s^{-1} for larvae <7.5 mm and 5.0×10^{-4} µmol m^{-2} s^{-1} for larvae ≥7.5 mm. Active metabolism, $metab_a$ (µg), was

$$metab_a = 1.4 \cdot metab_r \quad [20]$$

for larvae ≤5.5 mm and

$$metab_a = 2.5 \cdot metab_r \quad [21]$$

for larvae >5.5 mm.

Maximum growth

If the gut contents were enough for maximum growth ($gut \geq D$), then the mass specific growth rate (% d^{-1}) was a temperature-dependent rate,

$$sgr_{\max} = s_1 + s_2 \cdot T - s_3 \cdot T \cdot \ln(m_{mg}) - s_4 \cdot T \cdot \ln(m_{mg})^2 + s_5 \cdot T \cdot \ln(m_{mg})^3 \quad [22]$$

where s's are constants. The maximum instantaneous growth rate g_{max} (dt^{-1}) was calculated from the specific growth rate,

$$g_{max} = \ln\left(\left(\frac{sgr_{max}}{100}\right) + 1\right) \cdot dt/(24 \cdot 3600). \quad [23]$$

The biomass required to grow at the maximum rate, D (µg), was

$$D = (\exp(g_{\max}) - 1) \cdot m_{\mu g} + metab_a. \quad [24]$$

If $gut \geq D$, then the gut contents were reduced by D,

$$gut = gut - D, \quad [25]$$

the weight gain, $gain$ (µg), was

$$gain = (\exp(g_{\max}) - 1) \cdot m_{\mu g}, \quad [26]$$

and growth, g (dt^{-1}), was set as

$$g = g_{\max}. \quad [27]$$

Food-limited growth

If the gut contents were lower than required (*gut*<*D*) by the maximum growth, then growth was determined by the biomass available in the stomach. The weight gain equaled

$$gain = gut - metab_a, \quad [28]$$

and the gut contents were reduced by this amount

$$gut = gut - gain. \quad [29]$$

Instantaneous growth was calculated as

$$g = \ln(m_{\mu g} + gain) - \ln(m_{\mu g}). \quad [30]$$

Size increase

The larval weight was updated by the mass gained,

$$m_{\mu g} = m_{\mu g} + gain. \quad [31]$$

Length was calculated from weight as

$$l = \frac{m_{\mu g}{}^{1/3.768}}{0.194} \quad [32]$$

if this length was greater than or equal to the old length, otherwise the length from the previous time step was used since shrinking in length is not possible.

Starvation

A larva was considered to have starved to death if its mass fell below 70% of the reference mass, m_{ref} (µg), the mass that it would have at that length from an empirical length-weight relationship of haddock larvae;

$$m_{ref} = 0.194 \cdot l^{3.768}. \quad [33]$$

Predation submodel

The nonvisual predation rate, $pred_{nv}$ (dt^{-1}), was found using a size-dependent model adapted from Peterson and Wroblewski (1984)

$$pred_{nv} = 2.63 \cdot 10^{-4} \cdot m_g^{-0.25} \cdot dt/3600, \quad [34]$$

with larval mass, m_g, in g.

Visual predators were simulated by following the visual predation models of Aksnes and Giske (1993), Aksnes and Utne (1997), and Fiksen & Jørgensen (2011). Similar to larval vision, predator vision was a function of prey contrast, larval prey image area, A_l (m^2), predator eye sensitivity, E_p, the scattering of image-forming light, in situ light, and the light half saturation of the predator, K_e (µmol m^{-2} s^{-1}). Prey (larval fish) width was assumed to be a constant 20% of its length such that the equation for image area simplified to

$$A_{larva} = 0.75 \cdot l \cdot 0.2 \cdot l = 0.15 \cdot l^2. \quad [35]$$

The perception radius of a predator, R_{pred} (mm), increased with larval fish size as

$$R_{pred}^2 = C \cdot A_{larva} \cdot E_p \cdot \exp(-cR_{pred}) \cdot \frac{E(z)}{K_e + E(z)}. \quad [36]$$

Visual predator density N_{vis} (m^{-3}) was assumed to decrease with increasing larval size;

$$N_{vis} = 1.36 \cdot 10^{-2} \cdot m_{\mu g}^{-1}. \quad [37]$$

The visual predation rate, $pred_{vis}$ (dt^{-1}), took the form of that for a cruising fish predator,

$$pred_{vis} = 1800 \cdot \pi \cdot v \cdot R_{pred}^2 \cdot N_{vis} \cdot dt \ , \quad [38]$$

where v (m s^{-1}) was a constant that accounted for predator velocity, converting perception radius from mm to m, and a parameterization such that the total base predation rate was approximately 0.1 d^{-1} for a 5 mm larva (Bailey & Houde, 1989). The visual predation rate decreased with larval size and depth.

The total base predation rate, $pred_{base}$ (dt^{-1}), was the sum of nonvisual and visual predation rates,

$$pred_{base} = pred_{vis} + pred_{nv} \ . \quad [39]$$

Temperature dependent predation

In the alternate simulations, temperature-dependent predation, $pred_{temp}$ (dt^{-1}), was modeled as a 0.01 d^{-1} per 1°C increase in temperature following Houde (1989). The base predation rate was the constant rate used in the reference simulations.

$$pred_{temp} = pred_{base} + 0.01 \cdot (T - T_{base}) \quad [40]$$

In the T6 simulation, the base temperature, T_{base} (°C), was set as 6.5°C, the temperature associated with the predation rate of 0.1 d^{-1} for a 5 mm larva (Jones, 1973; Bailey & Houde, 1989; Houde, 1989);

$$pred_{temp} = pred_{base} + 0.01 \cdot (T - 6.5). \quad [41]$$

In the T5 simulation, T_{base} was lowered to 5.5°C to cause greater predation rates during warmer months,

$$pred_{temp} = pred_{base} + 0.01 \cdot (T - 5.5). \quad [42]$$

Spatially-dependent predation

Two different simulations were run with spatially-dependent predation. In each, the base predation rate was increased 50% in one location and decreased 50% in the other, resulting in a predation rate that was three times greater in one area than the other. In the higher crest predation simulation (CP), predation shoalward of the 60 m isobath, $pred_{crest}$ (dt^{-1}), and predation in waters deeper than 60 m, $pred_{flanks}$ (dt^{-1}), were

$$pred_{crest} = 1.5 \cdot pred_{base} , \quad [43]$$

$$pred_{flanks} = 0.5 \cdot pred_{base} . \quad [44]$$

In the opposite simulation with higher predation on the flanks (FP) the rates were

$$pred_{crest} = 0.5 \cdot pred_{base} , \quad [45]$$

$$pred_{flanks} = 1.5 \cdot pred_{base} . \quad [46]$$

Interannually varying predation

Another set of simulations varied the predation rates between years. The base predation rate was altered by ±10% in one year and by ±10% in the opposite direction in the other. 10% higher in 1995, 10% lower in 1998 (95+ or P+),

$$pred_{95} = 1.1 \cdot pred_{base} , \quad [47]$$

$$pred_{98} = 0.9 \cdot pred_{base}, \quad [48]$$

10% lower in 1995, 10% higher in 1998 (95- or P-),

$$pred_{95} = 0.9 \cdot pred_{base} , \quad [49]$$

$$pred_{98} = 1.1 \cdot pred_{base}, \quad [50]$$

Predation mortality losses

202 Losses of individuals within a super-individual via predation, n_{pred}, were modeled
203 for each super-individual by drawing a random number from a binomial distribution of
204 the current number of individuals, n, with the probability of predation, p.

205 $$n_{pred} \sim \text{binomial}(n, p). \quad [51]$$

206 The probability was calculated from an exponential probability distribution from the total
207 predation rate,

208 $$p = 1 - \exp(-pred_{base}). \quad [52]$$

209 This probability was used with an exact binomial probability density function when
210 $n \leq 20$. When $n > 20$ and $np \leq 50$, the Poisson approximation for a binomial distribution with
211 small p was used,

212 $$n_{pred} \sim \text{Poisson}(n \cdot p). \quad [53]$$

213 The Poisson distribution was further approximated by a normal distribution when $n > 20$
214 and $np > 50$,

215 $$n_{pred} \sim \text{normal}(n \cdot p, n \cdot p). \quad [54]$$

216 At each time step, the number of individuals was reduced by the number drawn from the
217 binomial or binomial approximated probability distribution,

218 $$n_t = n_{t-dt} - n_{pred}. \quad [55]$$

219

220 *Swimming behavior*

221 The diel vertical behavior simulations imposed preferred daytime and nighttime
222 depths of 40 m and 20 m, respectively, for larvae >9 mm following observations. Vertical
223 swimming velocity, w (m s $^{-1}$), was implemented as a tangential function that directed
224 larvae towards the preferred depth, z_{pref} (m);

$$w = w_{max} + \tanh\left(z - z_{pref}\right), \quad [56]$$

where w_{max} (m s^{-1}) was 1.5 times the routine swimming speed of larval cod,

$$w_{max} = 1.5 \cdot 10^{-3} \cdot (0.261 \cdot l^{1.552 \cdot l^{-0.08}} - \frac{5.289}{l}). \quad [57]$$

Table A1. Descriptions, units, values, and sources of symbols used in model equations.

Symbol	Description	Units	Value	Source
A_{cope}	copepod image area	mm^2	eq. 4	Kristiansen *et al.* (2007)
A_{larva}	larval image area	mm^2	eq. 35	Fiksen & Jørgensen (2011)
assim	assimilation efficiency	-	eq. 17	Lough *et al.* (2005)
att	light attenuation coefficient	m^{-1}	0.18	Kristiansen *et al.* (2007)
biom	copepod biomass	µg	Table A2	Davis (1984, 1987)
C	prey contrast	-	0.3	Aksnes & Utne (1997)
c	image-forming light attenuation	mm^{-1}	$5.4 \cdot 10^{-4}$	Aksnes & Giske (1993)
cap	number of each copepod stage captured	-	eq. 14	
D	biomass needed for maximum growth	µg	eq. 24	Kristiansen *et al.* (2007)
d_1	capture fit constant	-	$-1.06 \cdot 10^3$	
d_2	capture fit constant	-	$3.86 \cdot 10^3$	
d_3	capture fit constant	-	$-4.96 \cdot 10^2$	
d_4	capture fit constant	-	20.2	
dt	biological model time step	s	3600	
E_l	larval eye sensitivity	-	eq. 8	Fiksen & MacKenzie (2002)
E_p	predator eye sensitivity	-	$5 \cdot 10^4$	Fiksen & Jørgensen (2011)
E(z)	light	µmol m^{-2} s^{-1}	eq. 7	
ENCA	population model copepod density	m^{-3}	ENCA output	Ji *et al.* (2009)
enc	number encountered	-	eq. 13	MacKenzie & Kiørboe (1995)
f	pause frequency	s^{-1}	0.53	MacKenzie & Kiørboe (1995)
g	instantaneous growth rate	dt^{-1}	eqs. 27, 30	
g_{max}	maximum instantaneous growth rate	dt^{-1}	eq. 23	
gain	weight gain from growth	µg	eqs. 26, 28	Kristiansen *et al.* (2007)

gut	larval gut contents	µg	eqs. 18, 25, 29	Kristiansen *et al.* (2007)
i	copepod developmental stage	-	N, C, A	
$ingest_i$	biomass ingested of each stage	µg	eq. 15	
$ingest_{tot}$	total copepod biomass ingested	µg	eq. 16	
K_e	light half saturation	µmol m^{-2} s^{-1}	1.0	Aksnes & Utne (1997)
kh	vertical diffusivity	m^2 s^{-1}	FVCOM output	
l	larval length	mm	eq. 32	Lankin *et al.* (2008)
l_{cope}	copepod length	mm	Table A2	Davis (1984, 1987)
m_g	larval mass	g	$m_{\mu g} \cdot 10^{-6}$	
m_{ref}	larval reference mass	µg	eq. 33	Lankin *et al.* (2008)
$m_{\mu g}$	larval mass	µg	eq. 31	
m_{mg}	larval mass	mg	$m_{\mu g} \cdot 10^{-3}$	
$metab_a$	active metabolism	µg	eqs. 20, 21	Lough *et al.* (2005)
$metab_r$	routine metabolism	µg	eq. 19	Lankin *et al.* (2008)
N_{vis}	visual predator density	m^{-3}	eq. 37	
n	number of individuals per super-individual	-	eq. 55	
n_{pred}	number of individuals lost to predation	-	eqs. 51, 53, 54	Scheffer *et al.* (1995)
ω	turbulent velocity	mm s^{-1}	eq. 11	MacKenzie & Leggett (1993)
PAR	surface light	µmol m^{-2} s^{-1}	eq. 6	
p	predation probability	-	eq. 52	
p_{cap}	capture success probability	-	eq. 12	
$pred_{95}$	predation rate specific to 1995	dt^{-1}	eqs. 47, 49	
$pred_{98}$	predation rate specific to 1998	dt^{-1}	eqs. 48, 50	
$pred_{base}$	reference predation mortality rate	dt^{-1}	eq. 39	
$pred_{crest}$	predation mortality rate on crest	dt^{-1}	eqs. 43, 45	
$pred_{flanks}$	predation mortality rate on flanks	dt^{-1}	eqs. 44, 46	

$pred_{nv}$	nonvisual predation mortality rate	dt^{-1}	eq. 34	Peterson & Wroblewski (1984)
$pred_{temp}$	temperature-dependent predation mortality rate	dt^{-1}	eqs. 40, 41, 42	
$pred_{vis}$	visual predation mortality rate	dt^{-1}	eq. 38	Fiksen & Jørgensen (2011)
$prey_{dens}$	copepod density	mm^{-3}	eqs. 1, 2, 3	
R_{larva}	larval perception distance	mm	eq. 9	Aksnes & Utne (1997)
R_{pred}	predator perception distance	mm	eq. 36	Aksnes & Utne (1997)
r	prey:larva length ratio	-	l_{cope}:l	
s_1	maximum growth constant	$\% \ d^{-1}$	1.08	Folkvord (2005)
s_2	maximum growth constant	$\% \ d^{-1} \ °C^{-1}$	1.79	Folkvord (2005)
s_3	maximum growth constant	$\% \ d^{-1} \ °C^{-1} \ mm^{-1}$	0.074	Folkvord (2005)
s_4	maximum growth constant	$\% \ d^{-1} \ °C^{-1} \ mm^{-2}$	0.0965	Folkvord (2005)
s_5	maximum growth constant	$\% \ d^{-1} \ °C^{-1} \ mm^{-3}$	0.0112	Folkvord (2005)
sgr_{max}	maximum specific growth rate	$\% \ d^{-1}$	eq. 22	Folkvord (2005)
swrad	short wave radiation	$\mu mol \ m^{-2} \ s^{-1}$	FVCOM output	
τ	pause duration	s	1.4	MacKenzie & Kiørboe (1995)
T	temperature	°C	FVCOM output	
T_{base}	base temperature	°C	T6:6.5, T5:5.5	
tke	turbulent kinetic energy	$m^2 \ s^{-3}$	eq. 10	Davis *et al.* (1991)
u	copepod swimming speed	$mm \ s^{-1}$	eq. 5	Petrik *et al.* (2009)
v	visual predator constant	$m \ s^{-1}$	0.05	
w	larval swimming speed	$m \ s^{-1}$	eq. 56	
w_{max}	maximum larval swimming speed	$m \ s^{-1}$	eq. 57	Peck *et al.* (2006)
width	copepod width	mm	Table A2	Davis (1984, 1987)
z	larval depth	m		
z_{pref}	preferred depth for vertical behavior	m	day:40 m, night:20 m	Lough & Potter (1993)

249

Table A2. Mean copepod properties (Davis 1984, 1987).

	Developmental stage		
	N	C	A
l_{cope} (mm)	0.2850	0.6340	1.000
width (mm)	0.1483	0.3040	0.4000
biom (μg)	0.5767	4.040	16.67

APPENDIX 2: Particle number sensitivity analysis

METHODS

We randomly subsampled the model output with 3x particles to mean values and standard deviations for numbers of particles not simulated, and to see how modeled results compared to these. The reference cases for 1995 and 1998 were used as the model output. This output was randomly subsampled 100 times for each number of particles. We tested from 250 to the maximum number of particles of each cohort at intervals of 250. Model simulation results, subsampling mean ±1 s.d., and ±1 s.d. of the maximum number of particles subsampled were plotted against the number of particles. We defined convergence as when the mean fraction fell within ±1 s.d. of the maximum number of particles subsampled.

RESULTS

The mean fractions lost to the different sources of mortality and fractions survived appeared robust for particles ≥1000 in all cohorts of both years (Fig. A1-A4). However, model results with the original number of particles often fell outside of ±1 s.d. of the subsampled results (14/24 times). The subsample means were always within ±1 s.d. of the maximum number of particles subsampled for particle numbers ≥2250. Simulations with 3x the original number of particles always fell within ±1 s.d. of the maximum number of particles subsampled.

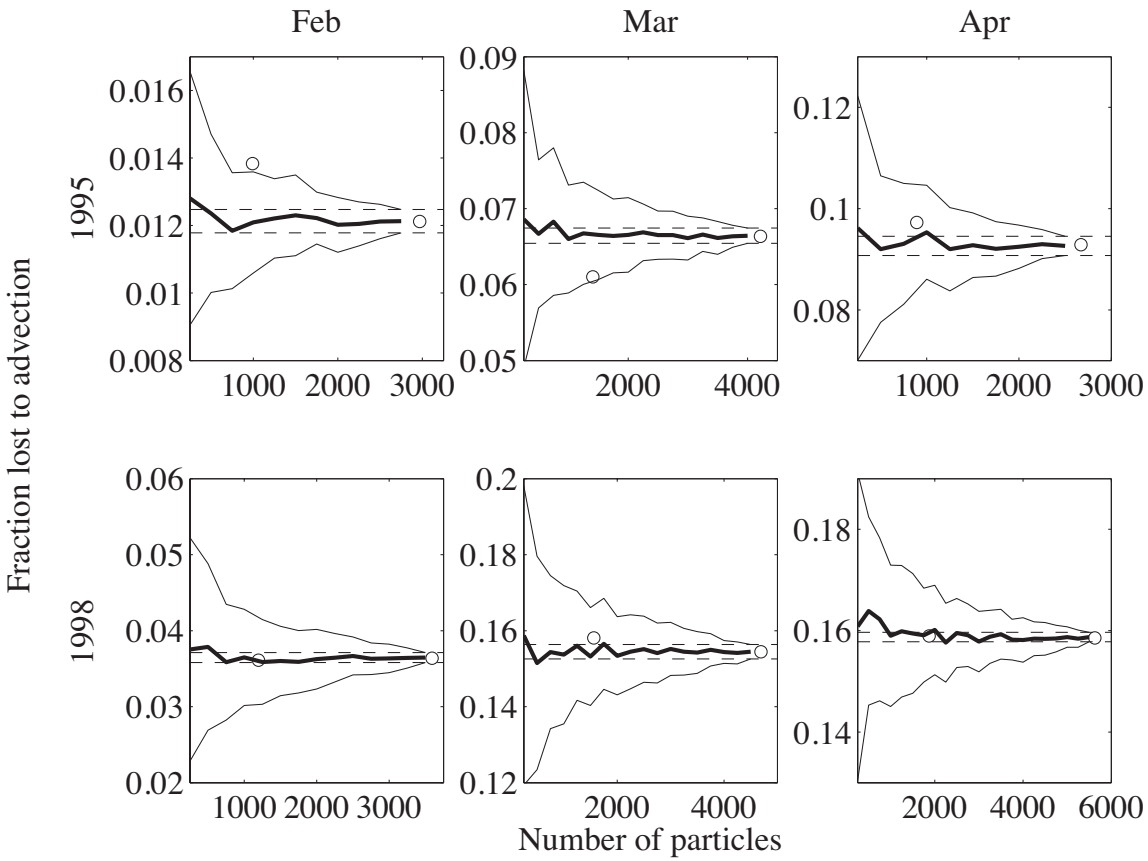

Fig. A1. Fraction of individuals lost to advection as a function of the number of particles simulated or subsampled. Heavy line: mean of 100 subsamples, thin line: ±1 s.d. of 100 subsamples, dashed line: ±1 s.d. of maximum number of particles subsampled for that cohort, circles: model simulations with 1x and 3x the original number of particles.

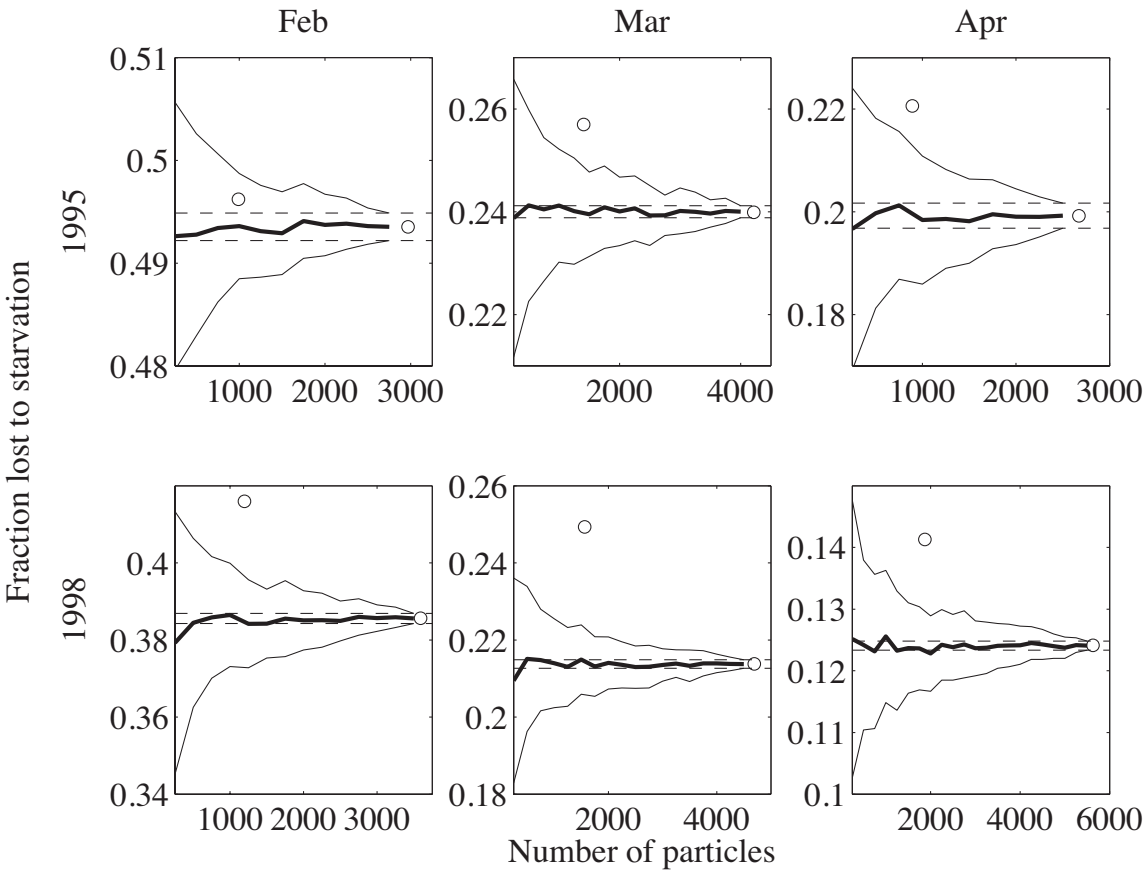

Fig. A2. Fraction of individuals lost to starvation as a function of the number of particles simulated or subsampled. Heavy line: mean of 100 subsamples, thin line: ±1 s.d. of 100 subsamples, dashed line: ±1 s.d. of maximum number of particles subsampled for that cohort, circles: model simulations with 1x and 3x the original number of particles.

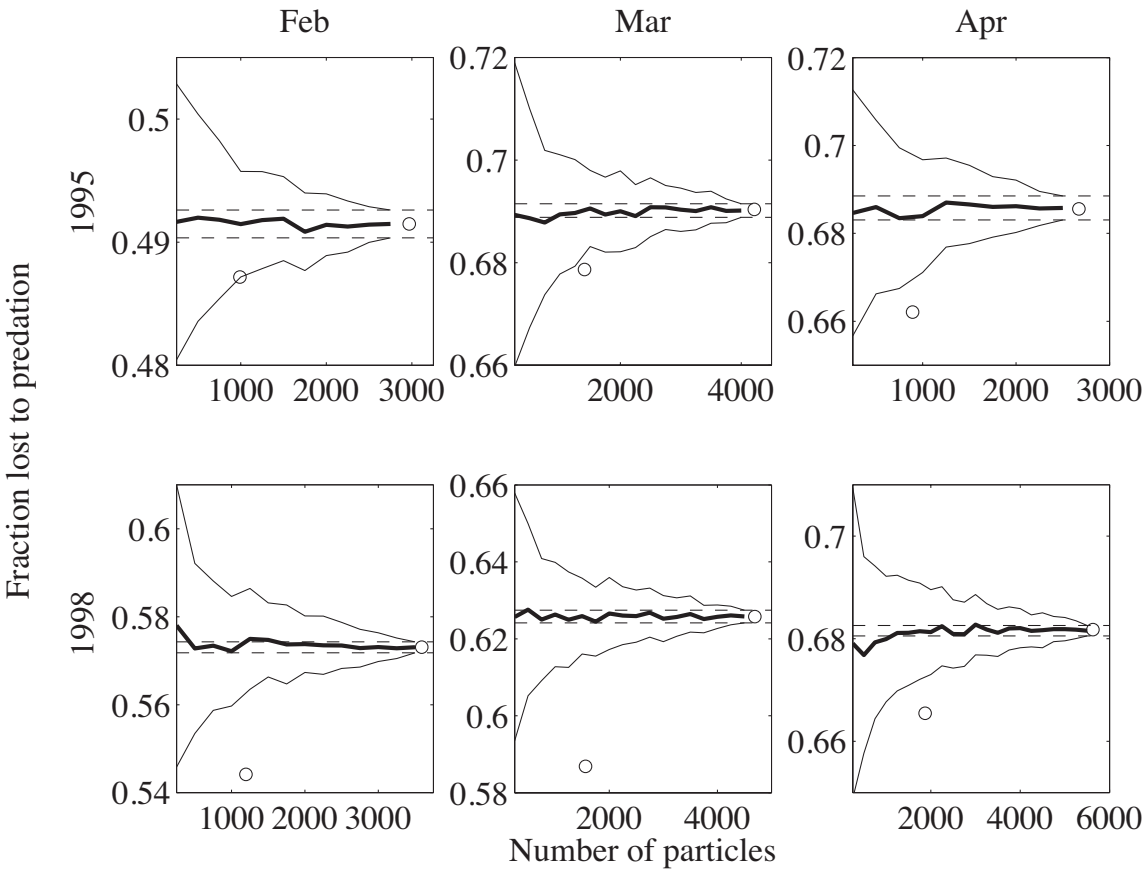

Fig. A3. Fraction of individuals lost to predation as a function of the number of particles simulated or subsampled. Heavy line: mean of 100 subsamples, thin line: ±1 s.d. of 100 subsamples, dashed line: ±1 s.d. of maximum number of particles subsampled for that cohort, circles: model simulations with 1x and 3x the original number of particles.

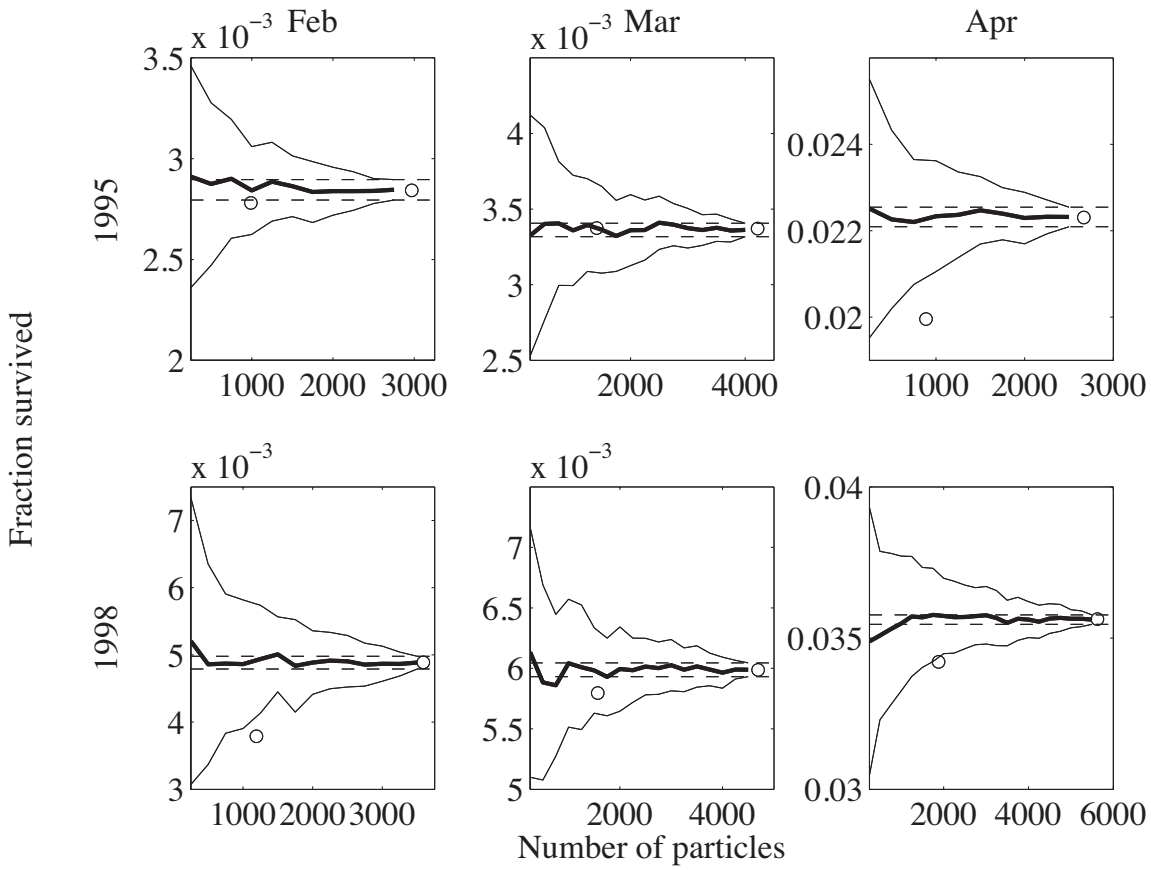

Fig. A4. Fraction of individuals that survived as a function of the number of particles simulated or subsampled. Heavy line: mean of 100 subsamples, thin line: ±1 s.d. of 100 subsamples, dashed line: ±1 s.d. of maximum number of particles subsampled for that cohort, circles: model simulations with 1x and 3x the original number of particles.